This is the author's unpublished manuscript.

Radiative transfer in interacting media

J. Kenneth Shultis

How to cite this manuscript

If you make reference to this manuscript, use the following information:

Shultis, J. K. (1998). Radiative transfer in interacting media. Retrieved from http://krex.ksu.edu

This item was retrieved from the K-State Research Exchange (K-REx), the institutional repository of Kansas State University. K-REx is available at http://krex.ksu.edu

Radiative Transfer in Interacting Media

J.Kenneth Shultis

Dept. Mechanical and Nuclear Engineering
Kansas State University
Fall 1998

1 Introduction

Radiative transfer began as a mathematical theory with Rayleigh's efforts (1871) to determine the distribution of sunlight in earth's atmosphere. At the turn of the century other scientists began to investigate the transmission of light through various media. Schuster and Schwartzschild (1905, 1906) formulated the radiative-equilibrium stellar-atmosphere problem and developed what is known today as the Schwartzschild-Milne equation. Lommel (1889) and Hvolson (1890) derived the same equation but in the context of light scattering in translucent media. From the period 1910 to about 1940, radiative transfer was developed as a discipline primarily by astronomers for whom detailed light measurements are the keystone to their science. Beginning in the 1940's and continuing to this day, developments in radiative transfer have been accelerated by neutron and high-energy photon transport methods for both military and civilian applications of nuclear energy.

Today, radiative transport plays an important role in many other areas besides nuclear and astronomical studies. Applications include: illumination and photometry in cloudy or foggy media, interpretation of many optical phenomena and spectroscopic analyses, radiation hydrodynamics in which radiation can affect the fluid flow (e.g., shock phenomena), energy loss from thermonuclear plasmas, combustion studies, and many others.

1.1 Radiative Transfer Regimes

The transport of radiant energy through a medium falls into three broad categories.

Short Wavelength Radiation: For high energy gamma and X rays ($\lambda \leq 10^{-3}\mu$m), the "size" of the radiation photons is less than that of atoms, and radiation mostly interacts with individual electrons or nuclei of the medium. Moreover, the intensity of the radiation field is generally sufficiently low that the radiation does not affect the optical properties of the medium. In this case, typical of many radiation shielding analyses, the radiative transfer equation is linear, and a wealth of numerical techniques exist to perform very accurate calculations of the radiation field.

Intermediate Wavelength Radiation: For infrared to soft X-rays (λ = 10^3 to $10^{-3}\mu$m) the radiation field is absorbed, scattered and reemitted both by individual atoms of the medium and also by small particles (e.g., soot, fog, etc.). In this regime, the radiation field often affects the optical properties of the medium, thereby making the radiative transfer equation inherently nonlinear.

Long Wavelength Radiation: For long wavelength radiation ($\lambda \geq 100\mu$m) the radiation is "large" compared to the size of atoms and particles composing the medium. Consequently, radar and radiowaves interact with all of the atoms in the medium simultaneously and the

concept of point interactions is no longer applicable. For such wavelengths, the radiation field is described by Maxwell's equations and not by the radiative transfer equation.

1.2 Differences Between Small and Intermediate Wavelength Regimes

In these notes, we consider radiative transfer in the first two of these regimes. The radiative transfer equation, which we will derive, applies equally to both of these wavelength regimes, and conceptually, we could treat both regimes in a single framework. However, the intermediate wavelength radiation presents much more of a challenge to the analyst than does the short wavelength case. Some of the properties which make the intermediate case more challenging are

- For intermediate wavelengths, the optical properties of the medium depend *strongly* on the radiation field. Thus, even though photon-photon interactions are ignored, the radiative transfer equation is highly nonlinear. At short wavelengths, the optical properties become independent of the radiation field, and the radiative transfer equation is linear.
- Optical properties, even for a homogeneous medium, generally vary continuously with position since the radiation field varies continuously with position. For short wavelengths, the optical properties usually depend only on the composition of the medium.
- Absorption and emission lines are numerous, very narrow, and occur over the whole spectrum of interest. By contrast, for short wavelength radiation the optical properties usually vary smoothly with radiation wavelength.
- For intermediate wavelengths, one often is interested in the *inverse problem*, i.e. given some measurements of the radiation field, one tries to determine some property of the medium. This is much more difficult than the *forward* problem of determining the radiation field at some point in the medium, which is the usual problem for the short wavelength radiation.

2 Radiation as Waves and Particles

For many phenomena radiant energy can be considered as electro-magnetic waves. Indeed Maxwell's equations, which describe very accurately long wave-length radiation interactions, immediately yield a wave equation for the electric and magnetic fields of radiant energy. Phenomena such as diffraction, interference, and other related optical effects can be described only by a wave model for radiation.

However, near the beginning of the twentieth century, several experiments involving light and X rays were performed that indicated that radiation also possessed particle-like properties. Today we understand through quantum theory that matter (e.g. electrons) and radiation (e.g., X-rays) both have wave-like and particle properties. This dichotomy, known as the *wave-particle duality principle* is a corner stone of modern physics. For some phenomena a wave description works best; for others, a particle model is appropriate. In this section, three pioneering experiments are reviewed that helped to establish the wave-particle nature of matter.

2.1 The Photoelectric Effect

In 1887, Hertz discovered that, when metal surfaces were irradiated with light, "electricity" was emitted. J.J. Thompson in 1898 showed that these emissions were electrons (thus the term *photo-electrons*). According to a classical (wave theory) description of light, the light energy was absorbed

by the metal surface, and when sufficient energy was absorbed to free a bound electron, a photoelectron would "boil" off the surface. If light were truly a wave, we would expect the following observations:

- Photoelectrons should be produced by light of all frequencies.
- The higher the light intensity (i.e. wave amplitude), the more energy is absorbed per second and hence the greater should be the photoelectron emission rate.
- At low intensities we would expect a time lag between the start of irradiation and the emission of a photoelectron since it takes time for the surface to absorb sufficient energy to eject an electron.
- The kinetic energy of the photoelectron should increase with the light intensity since more energy is absorbed by the surface.

However, experimental results different dramatically with these results. It was observed:

- For each metal there is a minimum light frequency below which no photoelectrons are emitted no matter how high the intensity.
- There is no time lag between the start of irradiation and the emission of photoelectrons, no matter how low the intensity.
- The intensity of the light affects only the emission *rate* of photoelectrons.
- The kinetic energy of the photoelectron depends only on the frequency of the light and not the intensity. The higher the frequency, the more energetic is the photoelectron.

In 1905 Einstein introduced a new light model which explained all these observations. Einstein assumed that light energy consisted on *photons* or "quanta of energy," each with an energy $E = h\nu$, where h is Planck's constant (6.62×10^{-20} J s) and ν is the light frequency. He further assumed that the energy associated with each photon interacts as a whole, i.e. either all the energy is absorbed by an atom or none is. With this "particle" model, the maximum energy of a photoelectron would be $E = h\nu - A$ where A the amount of energy required to free an electron from the metal. This if $h\nu < A$ no photoelectrons can be produced. Increasing the light intensity only increases the number of photons hitting the metal surface per unit time and thus the rate of photoelectron emission.

2.2 Compton Scattering

According to the wave model of electromagnetic radiation, radiation should be scattered from an electron equally in all directions with no change in wavelength. However, it 1922 Compton observed than x rays scattered from electrons had a decrease in the wavelength $\Delta\lambda = \lambda' - \lambda$ proportional to $(1 - \cos\theta_s)$ where θ_s was the scattering angle (see Fig. 1). To explain this observation, it was necessary to treat x rays as particles with a linear momentum $p = h/\lambda$ and energy $E = h\nu = pc$.

Since photons travel as the speed of light, we must use relativistic kinematics. According to Einstein's special theory of relativity, the total energy of a particle with speed v is

$$E = mc^2 = \frac{m_o}{\sqrt{1 - v^2/c^2}} \tag{1}$$

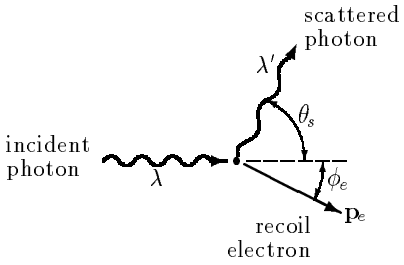

Figure 1. A photon with wavelength λ is scattering by an electron. After scattering, the photon has a longer wavelength λ' and the electron recoils with an energy T_e.

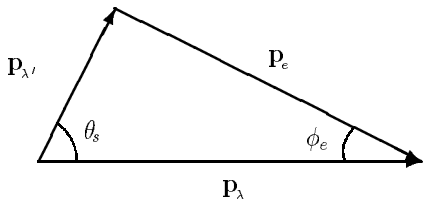

Figure 2. Conservation of momentum requires the initial momentum of the photon p_λ equal the sum of the momenta of the scattered photon and recoil electron.

where m_o is the *rest mass* (here, that of an electron) and m is its *relativistic mass*. The momentum p of a particle can be expressed in terms of these two masses, namely

$$p^2c^2 = (mc^2)^2 - (m_oc^2)^2. \tag{2}$$

In an x-ray scattering interaction, the energy and momentum before scattering must equal the energy and momentum after scattering. Conservation of linear momentum requires the initial momentum of the incident photon (the electron is assumed to be initially at rest) must equal the vector sum of the momenta of the scattered photon and the recoil electron. This requires the momentum vector triangle of Fig. 2 to be closed, i.e.

$$\mathbf{p}_\lambda = \mathbf{p}_{\lambda'} + \mathbf{p_e} \tag{3}$$

or from the law of cosines

$$p_e^2 = p_\lambda^2 + p_{\lambda'}^2 - 2p_\lambda p_{\lambda'} \cos\theta_s. \tag{4}$$

The conservation of energy requires

$$p_\lambda c + m_oc^2 = p_{\lambda'}c + mc^2 \tag{5}$$

which, with Eq. (2), can be rewritten as

$$p_\lambda + m_oc - p_{\lambda'} = \sqrt{p_e^2 + (m_ec)^2}. \tag{6}$$

Substitute for p_e from Eq. (4) into Eq. (6) and rearrange the result to obtain

$$\frac{1}{p_\lambda} - \frac{1}{p_{\lambda'}} = \frac{1}{m_oc^2}(1 - \cos\theta_s). \tag{7}$$

Then since $\lambda = h/p$, this result gives the decrease in the scattered wavelength as

$$\lambda' - \lambda = \frac{h}{m_oc}(1 - \cos\theta_s), \tag{8}$$

where $h/(m_oc) = 2.431 \times 10^{-6}\mu$m.

2.3 Electron Scattering

In 1924 de Broglie postulated that, since light had particle properties, then for symmetry, particles should have wave particles. Because photons had a discrete energy $E = h\nu$ and momentum $p = h/\lambda$, de Broglie suggested that a particle should have an associated wavelength $\lambda = h/p$.

Davisson and Germer in 1927 confirmed that electrons did indeed behave like waves with the de Broglie's predicted wavelength. In their experiment, shown schematically in Fig. 3, Davisson and Germer illuminated the surface of a Ni crystal by a perpendicular beam of 54-eV electrons and measured the number of electrons $N(\theta)$ reflected at different angles θ from the incident beam. According to the particle model, electrons should be scattered by individual atoms isotropically and $N(\theta)$ should exhibit no structure. However, $N(\theta)$ was observed to have a peak near 50° (see Fig. 4). This observation could only be explained by recognizing the peak as a constructive interference peak — a wave phenomena. Specifically, two reflected electron waves will be in phase (constructively interfere) in the difference in their path lengths AB in Fig. 3 is an integral number of wavelengths, i.e., if $d \sin\theta = n\lambda$, $n = 1, 2, \ldots$ where d is the distance between atoms of the crystal. This experiment and many similar ones clearly demonstrated that electrons (and other particles such as atoms) have wave-like properties.

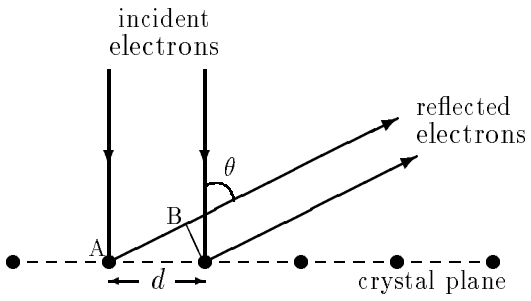

Figure 3. Electrons scattering from atoms on a crystalline plane, interfere constructively if the distance AB is a multiple of the electron's de Broglie wavelength.

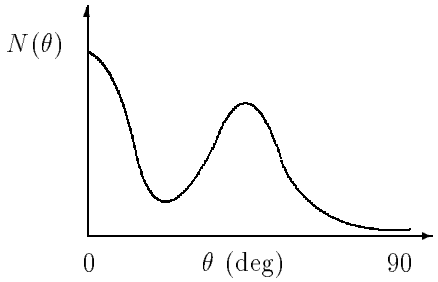

Figure 4. Observed number of electrons $N(\theta)$ scattered through an angle of θ degrees by the atoms in a nickel crystal.

3 Description of the Radiation Field

The rate at which radiant energy of a particular frequency flows through a medium is given by the *spectral intensity* $I_\nu(\mathbf{r}, \mathbf{\Omega}, t)$.[1] This fundamental description of the radiation field is defined such that $I_\nu(\mathbf{r}, \mathbf{\Omega}, t) d\Omega\, dt =$ the radiant energy traveling in directions $d\Omega$ about $\mathbf{\Omega}$ and with frequencies in $d\nu$ about ν that crosses a unit area perpendicular to $\mathbf{\Omega}$ in a time interval dt at time t. The spectral intensity I_ν is also sometimes referred to as the *radiation specific intensity* or the *angular spectral intensity*, and has units such as W m^{-2} sr^{-1} s^{-1}.

Equivalently, the radiation field is often described on a per-unit-wavelength basis by $I_\lambda(\mathbf{r}, \mathbf{\Omega}, t)$. The intensity in corresponding frequency and wavelength intervals must be equal so

$$I_\nu(\mathbf{r}, \mathbf{\Omega}, t) d\nu = -I_\lambda(\mathbf{r}, \mathbf{\Omega}, t) d\lambda. \tag{9}$$

[1] In Siegel and Howell, this quantity is denoted by $i'_\nu(\mathbf{r}, \theta, \psi, t)$.

Since $\lambda = c/\nu$,

$$I_\nu(\mathbf{r}, \mathbf{\Omega}, t) = I_\lambda(\mathbf{r}, \mathbf{\Omega}, t) \left[-\frac{d\lambda}{d\nu} \right] = I_\lambda(\mathbf{r}, \mathbf{\Omega}, t) \left[\lambda^2 / c \right] . \tag{10}$$

Once the spectral intensity $I_\nu()$ is known, many other useful measures of the radiation field can be derived. For example,

Average intensity:

$$J_\nu(\mathbf{r}, t) \equiv \frac{1}{4\pi} \int_{4\pi} d\Omega \, I_\nu(\mathbf{r}, \mathbf{\Omega}, t) \tag{11}$$

Radiant energy density:

$$u_\nu(\mathbf{r}, t) \equiv \frac{1}{c} \int_{4\pi} d\Omega \, I_\nu(\mathbf{r}, \mathbf{\Omega}, t) \tag{12}$$

Total energy density:

$$u(\mathbf{r}, t) \equiv \frac{1}{c} \int_0^\infty d\nu \int_{4\pi} d\Omega \, I_\nu(\mathbf{r}, \mathbf{\Omega}, t) \tag{13}$$

Radiant heat flux vector:

$$\mathbf{q}(\mathbf{r}, t) \equiv \int_0^\infty d\nu \int_{4\pi} d\Omega \, \mathbf{\Omega} I_\nu(\mathbf{r}, \mathbf{\Omega}, t) \tag{14}$$

Radiation pressure tensor:

$$\mathbf{P}(\mathbf{r}, t) \equiv \frac{1}{c} \int_0^\infty d\nu \int_{4\pi} d\Omega \, \mathbf{\Omega}\mathbf{\Omega} \, I_\nu(\mathbf{r}, \mathbf{\Omega}, t) \tag{15}$$

4 Optical Properties of the Medium

As radiation travels through a medium, it is absorbed and scattered. The absorbed energy is subsequently reemitted. In this section two basic material properties, the extinction and emission coefficients, are introduced. The physical processes that contribute to these coefficients are many and their relative importances depend upon the frequency of the radiation of interest. Discussion of these different physical processes is deferred to later sections; in this section, we restrict our presentation to defining these two coefficients, which play key role in radiative transfer, and to presenting some of their basic properties.

4.1 The Extinction Coefficient

Consider a plane-parallel beam of monoenergetic radiation normally incident on a slab of material with thickness Δx (see Fig. 5). The probability $P(\Delta x)$ that a photon interacts while trying to cross the slab equals the fractional decrease in the intensity caused by interactions (absorptions and scatters) in the slab, i.e.

$$P(\Delta x) = \frac{\Delta I_\nu^o}{I_\nu^o}. \tag{16}$$

It is observed empirically (see Fig. 6)

$$\lim_{\Delta x \to 0} \frac{P(\Delta x)}{\Delta x} = \text{constant} \equiv K_\nu. \tag{17}$$

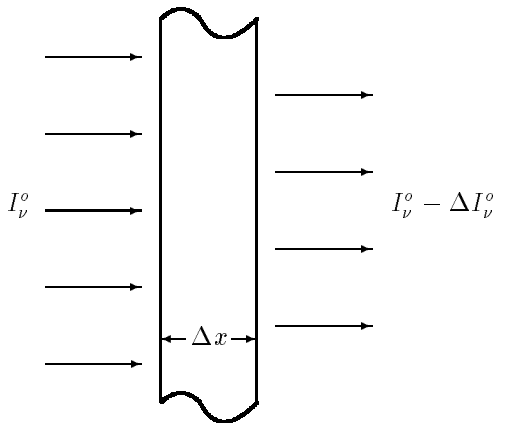

Figure 5. Radiation attenuated by a slab of thickness Δx.

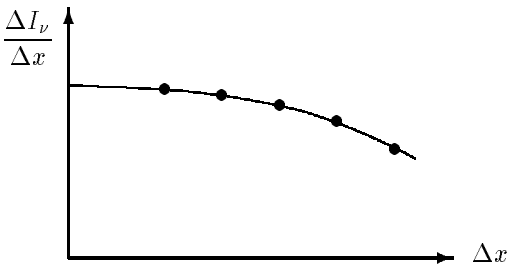

Figure 6. Measurement of interaction probability per unit slab thickness for different slab thicknesses.

The constant K_ν is called the *extinction coefficient*, which from Eq. (17), can be interpreted as the probability, per unit differential travel distance, a photon of frequency ν is absorbed or scattered. The extinction coefficient generally depends on the composition of the medium and on the local temperature and pressure. Since the radiation moving through a medium generally affects the temperature and pressure, K_ν will thus vary with position, even for a homogeneous medium.

4.1.1 Consequences of Eq. (17)

Consider a half space normally illuminated by monodirectional and monoenergetic radiation (see Fig. 7). At the slab surface the incident intensity is denoted by $I_\nu^o(0)$. As the radiation moves into the slab, the intensity of the original beam is attenuated so that $I_\nu^o(x)$ decreases as x increases. As the radiation crosses from x to $x + \Delta x$, the intensity decreases by an amount $I_\nu^o(x + \Delta x) - I_\nu^o(x)$. The probability a photon interacts while trying to cross the distance Δx is thus

$$P(\Delta x) = \frac{I_\nu^o(x + \Delta x) - I_\nu^o(x)}{I_\nu^o(x)}. \tag{18}$$

However, from Eq. (17)

$$K_\nu = \lim_{\Delta x \to 0} \frac{P(\Delta x)}{\Delta x} = \lim_{\Delta x \to 0} \left[\frac{I_\nu^o(x + \Delta x) - I_\nu^o(x)}{\Delta x} \right] \frac{1}{I_\nu^o(x)}. \tag{19}$$

In the limit, the term is square brackets becomes $dI_\nu^o(x)/dx$ so that the rate of change of radiation intensity with penetration depth is given by

$$\frac{I_\nu^o(x)}{dx} = -K_\nu I_\nu^o(x). \tag{20}$$

The solution of this differential equation for the given incident intensity $I_\nu^o(0)$ and for the special case that K_ν is constant is

$$I_\nu^o(x) = I_\nu^o(0) e^{-K_\nu x}. \tag{21}$$

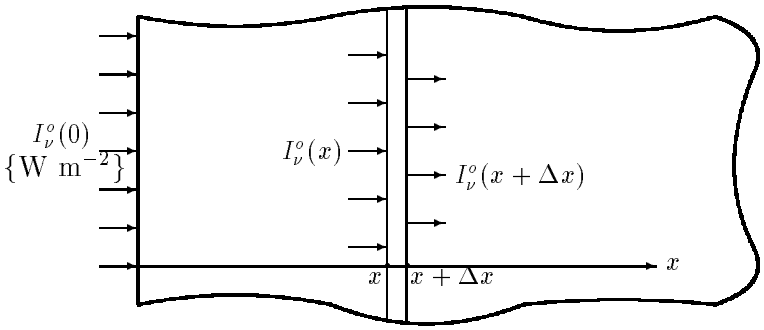

Figure 7. Attenuation of radiation as it penetrates a half space.

Thus it is seen that, in a medium with constant K_ν, radiation is *exponentially* attenuated. Also from this result, the probability of interaction in a finite distance x is seen to be

$$P(x) = 1 - \frac{I_\nu^o(x)}{I_\nu^o(0)} = 1 - e^{-K_\nu x}. \tag{22}$$

The probability of *not* interacting in a travel distance of x is thus

$$\overline{P}(x) = 1 - P(x) = e^{-K_\nu x}. \tag{23}$$

4.1.2 Radiation Mean Penetration Distance

To calculate the average distance photons travel before interacting (absorption or scatter), we need to determine the probability distribution function $p(x)dx$ which is the probability that a photon starting at $x = 0$ interacts for the first time in dx about x. Since a photon's fate is independent of its past history,

$$\begin{aligned} p(x)\,dx &= \{\text{prob. it travels dist. } x \text{ without interaction}\}\,\{\text{prob. it interacts in the next } dx\} \\ &= \left\{\overline{P}(x)\right\}\{P(dx)\} \\ &= \left\{e^{-K_\nu x}\right\}\left\{1 - e^{-K_\nu dx}\right\} \\ &= \left\{e^{-K_\nu x}\right\}\left\{1 - \left(1 - K_\nu dx + \frac{1}{2}K_\nu^2 dx^2 - \ldots\right)\right\} \\ &= K_\nu e^{-K_\nu x}\,dx \end{aligned} \tag{24}$$

Note that $\int_o^\infty p(x)dx = 1$ as required for a probability distribution function.

With this probability distribution function, the average distance a photon travels through a medium before interacting is found to be

$$t_m = \overline{x} \equiv \int_0^\infty dx\, x\, p(x) = K_\nu \int_0^\infty dx\, x\, e^{-K_\nu x} = \frac{1}{K_\nu}. \tag{25}$$

Thus, another interpretation of K_ν is that it is the inverse of the mean travel distance before interaction with the medium.

4.1.3 Half- and Tenth-Thickness

A closely related concept to the mean penetration distance, is the distance $x_{1/2}$ required for the radiation intensity to decrease to one-half of the initial intensity, i.e.,

$$\frac{I_\nu^o(x_{1/2})}{I_\nu^o(0)} = \frac{1}{2} = e^{-K_\nu x_{1/2}}. \tag{26}$$

Solving for $x_{1/2}$ yields

$$x_{1/2} = \frac{\ln 2}{K_\nu} \simeq \frac{0.693}{K_\nu}. \tag{27}$$

With a knowledge of $x_{1/2}$ it is a simple matter to determine the thickness of a material needed to reduce the radiation intensity to any desired level. For example, if the intensity is to be reduced by $1/2^n$, then a thickness $nx_{1/2}$ is required.

Similarly, the thickness required to attenuate the incident beam to one-tenth its initial value is

$$x_{1/10} = \frac{\ln 10}{K_\nu} \simeq \frac{2.30}{K_\nu}. \tag{28}$$

4.1.4 Attenuation with Variable K_ν

Generally, the extinction coefficient K_ν varies with position. In this case, radiation is still exponentially attenuated. The solution of Eq. (20) is

$$I_\nu^o(x) = I_\nu^o(0)e^{-\tau_\nu(x)} \tag{29}$$

where the *optical depth* or *opacity* is defined

$$\tau_\nu(x) \equiv \int_0^x K_\nu(x')\,dx'. \tag{30}$$

4.1.5 The Mass Extinction Coefficient

Extinction coefficients are often reported as $\kappa_\nu \equiv K_\nu/\rho$, the so-called *mass extinction coefficient.* The reason for this normalization is that, to a first approximation, we expect K_ν to be proportional to the atom (or particle) density in the medium, which, in turn, is proportional to the mass density ρ. Thus, the ratio K_ν/ρ should be relatively independent of the actual medium density.

4.2 The Emission Coefficient

The radiation energy absorbed at some point in a medium will generally be reradiated, albeit often at different wavelengths, very shortly after the absorption. We will go into detail later about the physical processes involved with this reemission of radiant energy. For the moment, the *emission coefficient* ϵ_ν is defined such that $\epsilon_\nu(\mathbf{r}, \mathbf{\Omega}, t)d\Omega\, d\nu\, dt$ is the radiant energy emitted per unit mass of material at $\mathbf{r}$ into directions $d\Omega$ about $\mathbf{\Omega}$ with frequencies in $d\nu$ about ν in a time interval dt at time t.

5 Derivation of the Radiative Transfer Equation

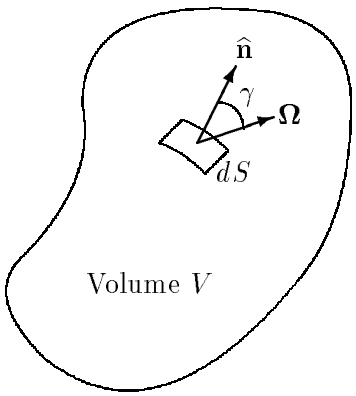

Figure 8. Arbitrary volume through whose surface radiation can freely pass.

The radiative transfer equation (RTE) describes how radiation migrates through an medium as it is scattered, absorbed, and reemitted by the various components of the medium. It can be derived by considering an energy balance in some *arbitrary* volume V surrounded by a closed surface S (see Fig. 8). Consider only the radiation energy in V that is traveling in directions $d\Omega$ about $\mathbf{\Omega}$ and with frequencies in $d\nu$ about ν. From an energy balance, the (a) rate of increase of such radiant energy in V must equal the rate of gain of these photons in V minus the rate of loss of photons with the specified direction and frequency.

Specifically, the following energy balance must hold

$$\left\{\begin{array}{l}\textbf{(a)}\text{ the rate of}\\ \text{increase of }(\nu,\mathbf{\Omega})\\ \text{radiant energy in }V\end{array}\right\} = -\left\{\begin{array}{l}\textbf{(b)}\text{ the net flow rate of}\\ (\nu,\mathbf{\Omega})\text{ radiation out of}\\ V\text{ across surface }S\end{array}\right\}$$
$$-\left\{\begin{array}{l}\textbf{(c)}\text{ rate at which}\\ (\nu,\mathbf{\Omega})\text{ radiant energy}\\ \text{is absorbed in }V\end{array}\right\}+\left\{\begin{array}{l}\textbf{(d)}\text{ rate at which }(\nu,\mathbf{\Omega})\\ \text{radiant energy is emitted}\\ \text{by the medium in }V\end{array}\right\}. \quad (31)$$

The four terms in this balance relation have the following interpretations: (a) is the rate of increase in the radiant energy due to photons with frequencies in $d\nu$ about ν and travelling in $d\Omega$ about $\mathbf{\Omega}$; (b) is the loss rate of radiant energy caused by the *net* flow of photons in $d\nu$ about ν in $d\Omega$ about $\mathbf{\Omega}$ that cross out of V minus that entering through the surface S; (c) is the rate at which energy in V in lost by photons in $d\nu$ about ν and in $d\Omega$ about $\mathbf{\Omega}$ being absorbed or scattered; and (d) is the rate of emission of radiant energy with frequencies in $d\nu$ about ν and traveling in $d\Omega$ about $\mathbf{\Omega}$.

The radiative transfer equation is obtained by expressing each term in this balance relation mathematically.

Term (a): The radiant energy density in a unit volume at $\mathbf{r}$ at time t due to photons with frequencies in $d\nu$ about ν and traveling in $d\Omega$ about $\mathbf{\Omega}$ is $I_\nu(\mathbf{r},\mathbf{\Omega},t)/c$. Thus differentiation, with respect to time, the volume-integrated energy density yields

$$\textbf{(a)} = \frac{d}{dt}\iiint_V dV\,\frac{I_\nu(\mathbf{r},\mathbf{\Omega},t)}{c}\,d\nu\,d\Omega = \frac{1}{c}\iiint_V dV\,\frac{\partial I_\nu(\mathbf{r},\mathbf{\Omega},t)}{\partial t}\,d\nu\,d\Omega. \quad (32)$$

Term (b): To calculate the net leakage of radiant energy through the surface S, consider those photons travelling in directions $d\Omega$ about $\mathbf{\Omega}$ through the element of the surface dS shown in Fig. 8. The surface element dS has a unit outward normal $\hat{\mathbf{n}}$ that makes an angle γ with the unit vector $\mathbf{\Omega}$. Note $\cos\gamma = \hat{\mathbf{n}}\bullet\mathbf{\Omega}$.

By definition, the energy flow through a unit area perpendicular to $\mathbf{\Omega}$ is just $I_\nu(\mathbf{r},\mathbf{\Omega},t)$. However, the energy flow through a unit area perpendicular to $\hat{\mathbf{n}}$ is less by a factor of $\cos\gamma$. Thus the leakage of radiation (with frequencies in $d\nu$ about ν and traveling in $d\Omega$ about $\mathbf{\Omega}$) is

$$\text{leakage through } dS = I_\nu(\mathbf{r},\mathbf{\Omega},t)\cos\gamma\, dS = \hat{\mathbf{n}}\bullet\mathbf{\Omega}\ I_\nu(\mathbf{r},\mathbf{\Omega},t). \tag{33}$$

If this quantity is positive, radiant energy flows out of V, while a negative result means energy flows into V. The net flow out of V is thus obtained by integrating this result over the entire surface, i.e.

$$\mathbf{(b)} = \iint_S dS\, \hat{\mathbf{n}}\bullet\mathbf{\Omega}\ I_\nu(\mathbf{r},\mathbf{\Omega},t)\, d\nu\, d\Omega. \tag{34}$$

Finally, this result can be converted to a volume integral by use of Gauss's divergence theorem, namely, for any continuous vector field $\mathbf{v}$ inside V

$$\iint_S dS\, \hat{\mathbf{n}}\bullet\mathbf{v}(\mathbf{r}) = \iiint_V dV\, \mathbf{\nabla}\bullet\mathbf{v}(\mathbf{r}). \tag{35}$$

Application of this theorem to Eq. (34) gives

$$\mathbf{(b)} = \iiint_V dV\, \mathbf{\nabla}\bullet\mathbf{\Omega}\ I_\nu(\mathbf{r},\mathbf{\Omega},t)\, d\nu\, d\Omega. = \iiint_V dV\, \mathbf{\Omega}\bullet\mathbf{\nabla} I_\nu(\mathbf{r},\mathbf{\Omega},t)\, d\nu\, d\Omega. \tag{36}$$

where the interchange of $\mathbf{\nabla}$ and $\mathbf{\Omega}$ in the last term is allowed since $\mathbf{\nabla}$ operates on only the spatial variable $\mathbf{r}$ and not on $\mathbf{\Omega}$.

Term (c): Consider radiation traveling in direction $\mathbf{\Omega}$ incident on a differential volume dV about the point $\mathbf{r}$. This differential volume presents a normal area dA and a depth ds to the incident beam so that $dV = dA\, ds$. Then, the rate at which radiant energy, with frequencies in $d\nu$ about ν and traveling in $d\Omega$ about $\mathbf{\Omega}$, interacts in dV (by absorption or scattering), and hence is removed from the photons under consideration, is

$$\begin{aligned}\text{energy interacting in } dV &= \{I_\nu\, d\Omega\, d\nu\, dA\}\{\text{prob. of interaction in distance } ds\}\\ &= \{I_\nu\, d\Omega\, d\nu\, dA\}\{\rho\kappa_\nu\, ds\}\\ &= \rho\kappa_\nu I_\nu(\mathbf{r},\mathbf{\Omega},t)\, d\Omega\, d\nu\, dV.\end{aligned} \tag{37}$$

Integration over all dV in V then yields

$$\mathbf{(c)} = \iiint_V dV\, \rho\kappa_\nu I_\nu(\mathbf{r},\mathbf{\Omega},t)\, d\Omega\, d\nu. \tag{38}$$

Term (d): By definition of the emission coefficient (see Section 4.1.5), the rate of radiant energy, with frequencies in $d\nu$ about ν and traveling in $d\Omega$ about $\mathbf{\Omega}$, that is emitted in V is

$$\mathbf{(d)} = \iiint_V dV\, \rho\epsilon_\nu(\mathbf{r},\mathbf{\Omega},t)\, d\Omega\, d\nu. \tag{39}$$

Now substitute Eqs. (32), (36), (38), and (39) into the balance relation of Eq. (31) and combining the integrals gives

$$\iiint_V dV\, \left\{\frac{1}{c}\frac{\partial I_\nu(\mathbf{r},\mathbf{\Omega},t)}{\partial t} + \mathbf{\Omega}\bullet\mathbf{\nabla} I_\nu(\mathbf{r},\mathbf{\Omega},t) + \rho\kappa_\nu I_\nu(\mathbf{r},\mathbf{\Omega},t) - \rho\epsilon_\nu\right\} = 0. \tag{40}$$

However, the volume V is arbitrary, and, hence, the integrand in this equation must itself be identically zero, i.e.,

$$\boxed{\frac{1}{c}\frac{\partial I_\nu(\mathbf{r},\mathbf{\Omega},t)}{\partial t} + \mathbf{\Omega}\bullet\nabla I_\nu(\mathbf{r},\mathbf{\Omega},t) = \rho[-\kappa_\nu I_\nu(\mathbf{r},\mathbf{\Omega},t) + \epsilon_\nu(\mathbf{r},\mathbf{\Omega},t)] = 0.} \tag{41}$$

This equation is the general form of the radiative transfer equation. Although it appears to be linear, it must be remembered that κ_ν and ϵ_ν usually are strong functions of the radiation field $I_\nu(\mathbf{r},\mathbf{\Omega},t)$, so that the RTE is usually highly nonlinear. As a consequence, analytic solutions are futile (except under highly unrealistic conditions), and even numerical solutions are usually quite difficult. Nevertheless, Eq. (41) is "exact" and forms the basis for the study of radiative heat transfer through interacting media.

5.1 Implicit Assumptions for the RTE

Although the above derivation of the RTE appears to be exact under very general conditions and geometry, there are several assumptions that have been implicitly made. These include

- We have assumed that the radiant energy in V is unpolarized. For polarized light, the spectral intensity I_ν is replaced by a 4-component vector of the Stoke's parameters that describe polarized radiation. Such an extension is beyond the scope of these notes; the interested reader is referred to *Radiative Transfer* by S. Chandrasekhar, Dover, NY, 1956.

- It has been assumed that radiation travels through a medium without dispersion, i.e., there is no dependence on the refractive index of the medium. Under this assumption, radiation (a photons) travels in a straight line between interactions.

- We have assumed there are no "collective" effects, i.e., there is no correlation among the scattering and absorption centers. In media with reflecting elements such as vegetative leaf canopies, this is not true, and radiation transport in such media is much more complicated.

- We have also assumed there are no external forces affecting the photon paths so that photons travel in straight lines. Near black holes, for example, this is not true.

- We have neglected photon-photon interactions so that Eq. (41) assumes an apparent linear form. Except under extreme conditions, such as those in certain cosmology models, this is generally valid. Nonetheless, even with this assumption, Eq. (41) is generally nonlinear for the reasons previously discussed.

5.2 The Streaming Term of RTE

Although the choice of the spatial and directional coordinate system is independent of the radiative transfer problem, geometric symmetries which may be present can often be more easily expressed in one coordinate system than another. If the problem has any spatial symmetry, a proper choice of the coordinate system usually allows the elimination of one or more of the independent spatial variables. Many coordinate systems are available, results are presented below for the three most commonly encountered ones: rectangular (Cartesian), spherical, and cylindrical.

The basic difficulty in writing the radiative transfer equation for a particular geometry is expressing the leakage or streaming term, $\mathbf{\Omega}\bullet\nabla I_\nu(\mathbf{r},\mathbf{\Omega},t)$, in terms of the variables of the coordinate

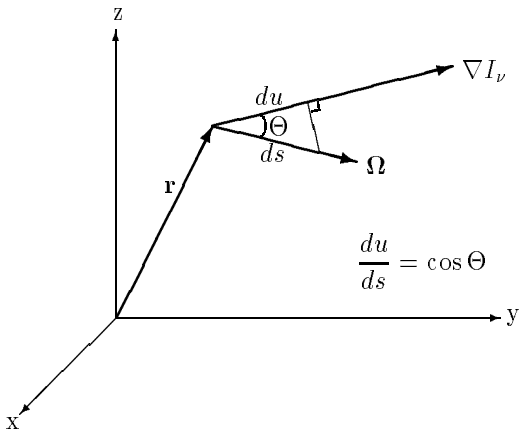

Figure 9. Orientation of the unit vector $\mathbf{\Omega}$ and the gradient of $\phi(\mathbf{r}, E, \mathbf{\Omega})$.

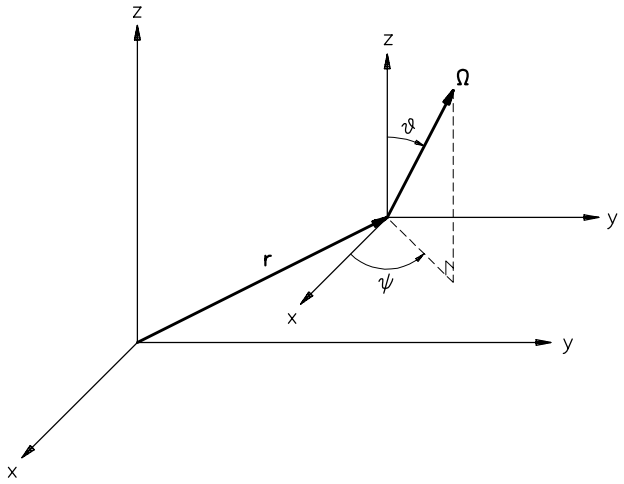

Figure 10. Rectangular coordinate system for $\mathbf{r}(x, y, z)$ and the spherical coordinate system used for $\mathbf{\Omega}(\theta, \psi)$.

system. Suppose that distances s and u are measured along the directions of $\mathbf{\Omega}$ and $\mathbf{\nabla}\phi$, as in Fig. 9, and that Θ is the angle between these two vectors. Then, since $\mathbf{\nabla} I_\nu = d\phi/du$, $du/ds = \cos\Theta$, and $\mathbf{\Omega}$ is a unit vector,

$$\mathbf{\Omega}\bullet\mathbf{\nabla} I_\nu = \cos\Theta \frac{dI_\nu}{du} = \cos\Theta \frac{ds}{du}\frac{dI_\nu}{ds} = \frac{dI_\nu}{ds}. \tag{42}$$

Thus $\mathbf{\Omega}\bullet\mathbf{\nabla} I_\nu(\mathbf{r},\mathbf{\Omega},t)$ is the rate of change of I_ν along the direction of particle travel $\mathbf{\Omega}$, namely, dI_ν/ds. To calculate the explicit expression for the streaming term $\mathbf{\Omega}\bullet\mathbf{\nabla} I_\nu$ in any geometry, one needs only to evaluate dI_ν/ds in terms of the spatial and angular variables of the particular geometry.

As an example, consider the Cartesian spatial coordinate system for $\mathbf{r}$ and spherical coordinate system for $\mathbf{\Omega}$ shown in Fig. 10. For this case, the streaming term is expressed as

$$\begin{aligned}\mathbf{\Omega}\bullet\mathbf{\nabla} I_\nu(\mathbf{r},\mathbf{\Omega},t) &= \frac{dI_\nu(x,y,z,\theta,\psi)}{ds}, \\ &= \frac{\partial I_\nu}{\partial x}\frac{dx}{ds} + \frac{\partial I_\nu}{\partial y}\frac{dy}{ds} + \frac{\partial I_\nu}{\partial z}\frac{dz}{ds} + \frac{\partial I_\nu}{\partial \theta}\frac{d\theta}{ds} + \frac{\partial I_\nu}{\partial \psi}\frac{d\psi}{ds}.\end{aligned} \tag{43}$$

From Fig. 10 the following variations of x, y, z, θ, and ψ with distance s along $\mathbf{\Omega}$ are found:

$$\begin{aligned}\frac{dx}{ds} &= \sin\theta\cos\psi = \sqrt{1-\omega^2}\cos\psi \\ \frac{dy}{ds} &= \sin\theta\sin\psi = \sqrt{1-\omega^2}\sin\psi \\ \frac{dz}{ds} &= \cos\theta = \omega\end{aligned}$$

and

$$\frac{d\theta}{ds} = \frac{d\psi}{ds} = 0,$$

where $\omega \equiv \cos\theta$. Thus, from Eq. (43) the streaming term becomes

$$\mathbf{\Omega}\bullet\mathbf{\nabla} I_\nu = \sqrt{1-\omega^2}\left(\cos\psi\frac{\partial I_\nu}{\partial x} + \sin\psi\frac{\partial I_\nu}{\partial y}\right) + \omega\frac{\partial I_\nu}{\partial z}. \tag{44}$$

For the special case in which the sources and material properties do not depend on x or y, the radiation intensity I_ν varies only with z, ω (or θ), and in general, ψ. Thus, the derivatives $\partial I_\nu/\partial x$ and $\partial I_\nu/\partial y$ in Eq. (44) vanish, and

$$\mathbf{\Omega}\bullet\mathbf{\nabla} I_\nu = \omega\frac{\partial I_\nu(z,\omega,\psi)}{\partial z}. \tag{45}$$

For other geometries the explicit form of the streaming term in the radiative transfer equation is more complicated. In Table 1, explicit forms for the streaming term are given for the three widely used geometries shown in Fig. 11.

6 Radiation Interactions with Matter

The manner in which electro-magnetic radiation interacts with matter depends on many factors, the most important of which are the *state* of the matter, i.e., whether gaseous or condensed (liquids and solids) and the *size* or wavelength of the radiation.

Table 1. Forms of the streaming term $\mathbf{\Omega}\bullet\nabla I_\nu$ in the three simplest orthogonal geometries.

Geometry	Spatial variables	Angular variables[a]	$\mathbf{\Omega}\bullet\nabla I_\nu$
Rectangular	z	ω	$\omega\dfrac{\partial I_\nu}{\partial z}$
	z, x	ω, η	$\omega\dfrac{\partial I_\nu}{\partial z} + \eta\dfrac{\partial I_\nu}{\partial x}$
	z, x, y	ω, η, ξ	$\omega\dfrac{\partial I_\nu}{\partial z} + \eta\dfrac{\partial I_\nu}{\partial x} + \xi\dfrac{\partial I_\nu}{\partial y}$
Cylindrical[b]	r	α, ξ	$\dfrac{\omega}{r}\dfrac{\partial (rI_\nu)}{\partial r} - \dfrac{1}{r}\dfrac{\partial (\eta I_\nu)}{\partial \alpha}$
	r, ϑ	α, ξ	$\dfrac{\omega}{r}\dfrac{\partial (rI_\nu)}{\partial r} + \dfrac{\eta}{r}\dfrac{\partial I_\nu}{\partial \vartheta} - \dfrac{1}{r}\dfrac{\partial (\eta I_\nu)}{\partial \alpha}$
	r, z	α, ξ	$\dfrac{\omega}{r}\dfrac{\partial (rI_\nu)}{\partial r} + \xi\dfrac{\partial I_\nu}{\partial z} - \dfrac{1}{r}\dfrac{\partial (\eta I_\nu)}{\partial \alpha}$
	r, ϑ, z	α, ξ	$\dfrac{\omega}{r}\dfrac{\partial (rI_\nu)}{\partial r} + \dfrac{\eta}{r}\dfrac{\partial I_\nu}{\partial \vartheta} + \xi\dfrac{\partial I_\nu}{\partial z} - \dfrac{1}{r}\dfrac{\partial (\eta I_\nu)}{\partial \alpha}$
Spherical[c]	r	ω	$\dfrac{\omega}{r^2}\dfrac{\partial (r^2 I_\nu)}{\partial r} + \dfrac{1}{r}\dfrac{\partial [(1-\omega^2) I_\nu]}{\partial \omega}$
	r, ϑ	ω, α	$\dfrac{\omega}{r^2}\dfrac{\partial (r^2 I_\nu)}{\partial r} + \dfrac{\eta}{r\sin\vartheta}\dfrac{\partial (\sin\vartheta I_\nu)}{\partial \vartheta} + \dfrac{1}{r}\dfrac{\partial [(1-\omega^2) I_\nu]}{\partial \omega} - \dfrac{\cot\vartheta}{r}\dfrac{\partial (\xi I_\nu)}{\partial \alpha}$
	r, ϑ, ψ	ω, α	$\dfrac{\omega}{r^2}\dfrac{\partial (r^2 I_\nu)}{\partial r} + \dfrac{\eta}{r\sin\vartheta}\dfrac{\partial (\sin\vartheta I_\nu)}{\partial \vartheta} + \dfrac{\xi}{r\sin\vartheta}\dfrac{\partial I_\nu}{\partial \psi} + \dfrac{1}{r}\dfrac{\partial [(1-\omega^2) I_\nu]}{\partial \omega} - \dfrac{\cot\vartheta}{r}\dfrac{\partial (\xi I_\nu)}{\partial \alpha}$

[a] The angles ϑ, ψ, and α are in radians.

[b] $\omega = \sqrt{1-\xi^2}\cos\alpha, \eta = \sqrt{1-\xi^2}\sin\alpha$; α is the angle of revolution about the $\widehat{\boldsymbol{\xi}}$ axis.

[c] $\eta = \sqrt{1-\omega^2}\cos\alpha, \xi = \sqrt{1-\omega^2}\sin\alpha$; α is the angle of revolution about the $\widehat{\boldsymbol{\omega}}$ axis.

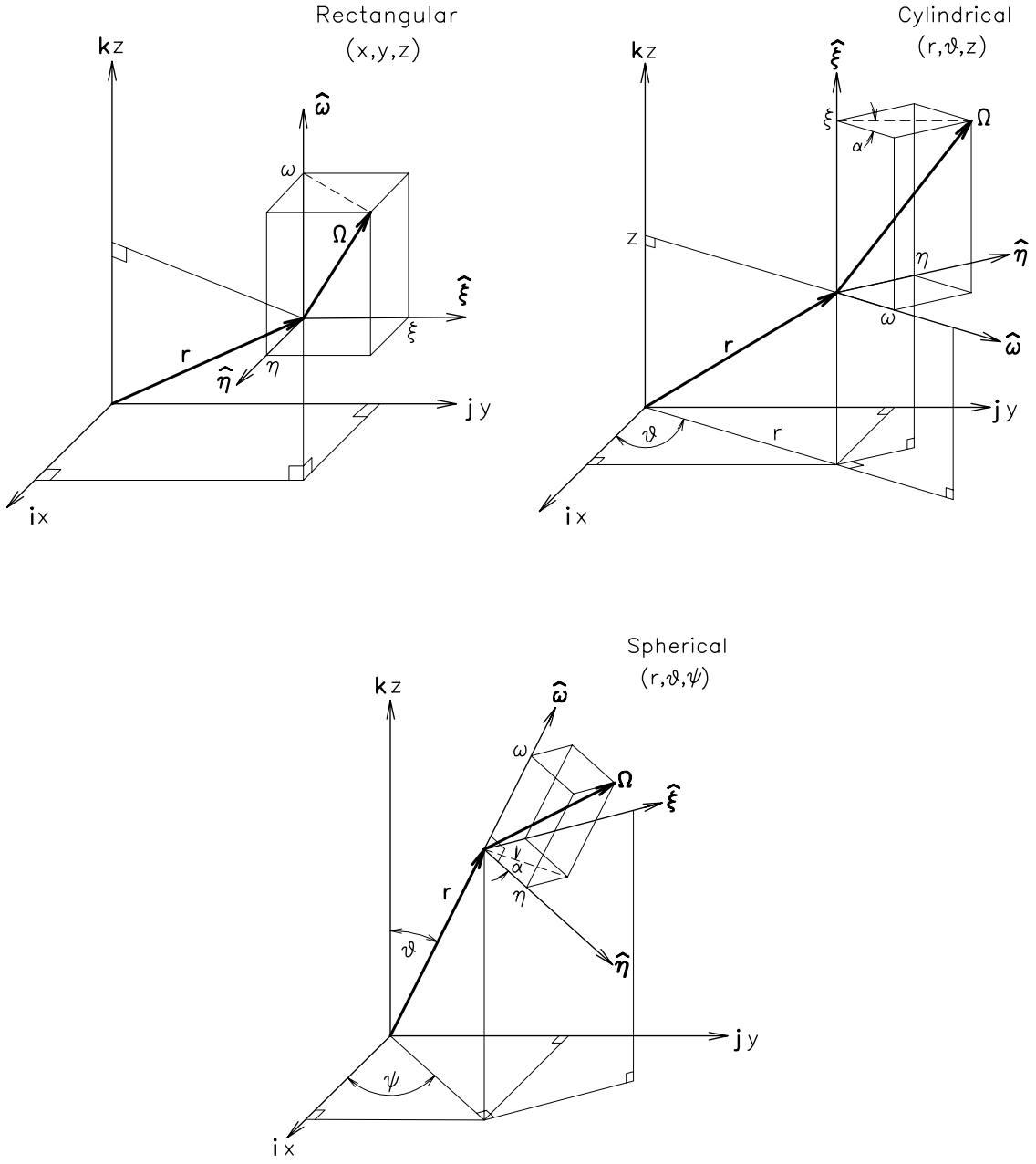

Figure 11. Coordinate systems for the three most commonly used geometries with the transport equation. The quantities $\widehat{\boldsymbol{\omega}}$, $\widehat{\boldsymbol{\eta}}$, and $\widehat{\boldsymbol{\xi}}$ are unit vectors for a local coordinate system (generally, functions of the position coordinate system) with respect to which exist the directional cosines $\omega = \widehat{\boldsymbol{\omega}} \cdot \boldsymbol{\Omega}$, $\eta = \widehat{\boldsymbol{\eta}} \cdot \boldsymbol{\Omega}$, and $\xi = \widehat{\boldsymbol{\xi}} \cdot \boldsymbol{\Omega}$.

For very long wavelengths (infrared and microwave) radiation, the photons have very small energy ($<<$ 1 eV) and are too "big" ($>>$ 1μm) to interact with orbital electrons of the atoms of the medium. Rather they interact at the molecular level where they can be absorbed to excite vibrational or rotational states of molecules. For media containing dust or colloidal particles, which are comparable in size to the radiation wavelength, the radiation can be strongly diffracted and scattered by the particles.

At shorter wavelengths (visible, ultraviolet, X rays, and gamma rays) radiation is comparable to the size of atoms (or even the nuclei of atoms) and interacts with atomic electrons (or even the nuclei). For such wavelengths the particle model of radiation is almost always used. Many photon-medium reactions are possible. Photons can scatter collectively from all the electrons of an atom/molecule (Raman scattering), remove an electron from an atom (a photoelectric or ionization interaction), scatter from an orbital electron (Compton scatter), or interact in the electric field of a nucleus to create an electron-positron pair. At very short wavelengths ($h\nu \geq 10$ MeV) photons interact with the atomic nuclei in a variety of ways producing secondary neutrons, protons, alpha-particles and such.

Radiation interactions with matter are categorized as "scatters" if a secondary photon is produced within about 10^{-10} s of the interaction. If the secondary photon has the same energy as the incident photon, the scatter is said to be *elastic*. By contrast, if the scattering interaction leaves the atom in an excited state, the scattered photon has less energy than the incident photon, and the scatter is termed *inelastic*.

6.1 Photon Reactions

For wavelengths of visible light and shorter, interactions can be categorized as a *scatter* (a secondary photon appears with negligible time delay) or as a *capture* if the photon energy is absorbed and reemitted at times after the interaction. All photon reactions contribute to the extinction coefficient κ_ν and those that produce a secondary photon contribute to the emission coefficient $\epsilon_n u$. Interactions contributing to κ_ν include:

Elastic Scatter:

1. *Rayleigh scattering:* scattering by atoms and molecules with negligible loss of photon energy. (bound–bound)
2. *Thomson scattering:* scattering by free electrons in the low energy limit. (bound–bound)
3. *Mie scattering:* scattering from large particles. Radiation is diffracted (constructively and destructively) around the particle.

Inelastic Scatter:

1. *Compton:* scattering from an atomic orbital electron. The recoil electron is freed from the atom. (bound-free)
2. *Raman:* scattering by atom or molecules (energy goes into internal excitation states. (bound-bound)

Capture:

1. *line absorption:* moves electron to higher energy orbital. (bound-bound)

2. *photoionization:* frees an electron from an atom. (bound–free)
3. *inverse Bremsstrahlung:* photon transfers energy to a free electron. (free–free)
4. *photodissociation:* photon breaks molecular bond.
5. *pair production:* photon interacts in the electric field near a nucleus and produced a positron-electron pair. This reaction occurs only if the incident photon energy is greater than 1.02 MeV.
6. *various nuclear reactions* incident photon is absorbed in a nucleus, excites it, and causes various particles to be emitted. Important only if photon energy $\geq$ 20 MeV.

6.2 Contributions to the Extinction and Emission Coefficients

Each capture process has an inverse that produces a photon and thus contributes to the emission coefficient ϵ_ν. Similarly, all scatters contribute to ϵ_ν. The inverse of capture processes may proceed *spontaneously* (i.e., the emission of the secondary photon occurs randomly with a characteristic decay time constant), or may be *induced*. In induced emission, an incident photon, with nearly the same frequency used to create the excited state, causes the atom or molecule to deexcite by emitting a photon in phase with the passing photon. Thus, in induced emission, one incident photon produces two photons, without any time delay and traveling in phase in the same direction.

For an isotropic medium the extinction coefficient K_ν is independent of $\mathbf{\Omega}$, the directional of the radiation interacting in the medium. By contrast, the emission coefficient ϵ_ν is usually highly anisotropic because of (1) induced emission which produces secondary photons in the direction of the incident radiation, and (2) anisotropic scattering.

Finally, since induced emission contributes to both the extinction coefficient (the incident photon interacts) and the emission coefficient (two photons are emitted with the same direction and phase of the incident photon), the contributions are often combined into a single negative contribution to the extinction coefficient. This can be done since no change in energy or direction occurs in the induced emission, only an increase in the number of photons. The resulting rearrangement of the right-hand side of Eq. (41) is shown below.

$$\begin{aligned}
\rho[-\kappa_\nu I_\nu + \epsilon_\nu] &= -\left\{\begin{array}{l}+\text{ capture of photon}\\ +\text{scatter from } (\nu,\mathbf{\Omega})\\ +\text{ inducing photon in}\end{array}\right\} + \left\{\begin{array}{l}+\text{ spontaneous emission}\\ +\text{ 2 induced photons out}\\ +\text{ scatter into } (\nu,\mathbf{\Omega})\end{array}\right\} \\
&= -\left\{\begin{array}{l}+\text{ capture of photon}\\ +\text{ scatter from } (\nu,\mathbf{\Omega})\\ -\text{ 1 induced photon}\end{array}\right\} + \left\{\begin{array}{l}+\text{ spontaneous emission}\\ +\text{ scatter into } (\nu,\mathbf{\Omega})\end{array}\right\} \\
&= \rho[-\kappa'_\nu I_\nu + \epsilon'_\nu] \qquad (46)
\end{aligned}$$

where κ'_ν and ϵ'_ν are called the *reduce* or *corrected* coefficients.

6.3 Absorption and Scattering Coefficients

The extinction coefficient K_ν can generally be decomposed into two components, $K_\nu = \mu_a + \mu_s$, where μ_a is the linear absorption coefficient and μ_s is the linear scattering coefficient. The total absorption coefficient is the sum of the absorption coefficients for all possible physical absorption processes, i.e. $\mu_a = \sum_i \mu_a^i$ where μ_a^i is the absorption coefficient for the ith absorption process. Similarly, the scattering coefficient can be decomposed as $\mu_s = \sum_i \mu_s^i$ where μ_s^i is the scattering coefficient for the ith scattering process.

6.4 Differential Scattering Coefficient and Phase Function

As listed in Section 6.1, there are several types of physical reactions that cause photons to be scattered as they move through a medium. To describe the scattering of photons, by the ith process, from an incident direction $\mathbf{\Omega}$ into another direction $\mathbf{\Omega}'$, the *phase function* p_i is used. This function is defined such that $p_i(\mathbf{r};\nu,\mathbf{\Omega}\rightarrow\nu',\mathbf{\Omega}')d\nu'\,d\Omega'$ is the probability that a photon with frequency ν and traveling in direction $\mathbf{\Omega}$, upon scattering by the ith process, has a frequency in $d\nu'$ about ν' and travels in $d\Omega'$ about $\mathbf{\Omega}'$. Such a phase function is normalized as[2]

$$\int_0^\infty d\nu' \int d\Omega'\, p_i(\mathbf{r};\nu,\mathbf{\Omega}\rightarrow\nu',\mathbf{\Omega}')d\nu'\,d\Omega' = 1. \tag{47}$$

The *differential scattering coefficient* $\mu_s^i(\mathbf{r};\nu,\mathbf{\Omega}\rightarrow\nu',\mathbf{\Omega}')d\nu'\,d\Omega'$ is defined as the probability, per unit differential path-length of travel, that a photon with frequency ν and direction $\mathbf{\Omega}$ scatters by the ith scattering process into $d\nu'$ about ν' and into a direction within $d\Omega'$ about $\mathbf{\Omega}'$. In terms of the phase function

$$\mu_s^i(\mathbf{r};\nu,\mathbf{\Omega}\rightarrow\nu'\mathbf{\Omega}') = \mu_s^i(\mathbf{r},\nu,\mathbf{\Omega},t)\,p_i(\mathbf{r};\nu,\mathbf{\Omega}\rightarrow\nu',\mathbf{\Omega}') \tag{48}$$

where $\mu_s^i(\mathbf{r},\nu,\mathbf{\Omega},t)$ is the total scattering coefficient for the ith scattering process.

6.4.1 Isotropic Medium and Other Simplifications

For an isotropic medium, the phase function depends on only the cosine of the scattering angle, $\omega_s \equiv \mathbf{\Omega}\bullet\mathbf{\Omega}' = \cos\theta\cos\theta' + \sin\theta\sin\theta' cos(\phi-\phi')$, and not on the individual directions $\mathbf{\Omega}(\theta,\phi)$ and $\mathbf{\Omega}'(\theta',\phi')$ separately. Thus

$$p_i(\mathbf{r};\nu,\mathbf{\Omega}\rightarrow\nu'\mathbf{\Omega}') \longrightarrow p_i(\mathbf{r};\nu,\rightarrow\nu',\mathbf{\Omega}\bullet\mathbf{\Omega}') = p_i(\mathbf{r};\nu,\rightarrow\nu',\omega_s). \tag{49}$$

Also, for an isotropic medium, the probability of scattering is independent of the photon direction $\mathbf{\Omega}$, so that the total scattering coefficient is a function only of position, frequency and, perhaps, time, i.e., $\mu_s^i(\mathbf{r},\nu,\mathbf{\Omega},t) \longrightarrow \mu_s^i(\mathbf{r},\nu,t)$. For the rest of this discussion, it is assumed that the medium under consideration is isotropic.

For some scattering processes (e.g., reflection from a dielectric sphere), there is no change in frequency, and $p_i(\mathbf{r};\nu,\rightarrow\nu',\omega_s) = \overline{p}_i(\mathbf{r},\nu,\omega_s)\delta(\nu-\nu')$, where the modified phase function $\overline{p}$ has the normalization

$$\int_{4\pi} d\Omega'\,\overline{p}_i(\mathbf{r},\nu,\omega_s)\,d\Omega' = 1. \tag{50}$$

The corresponding differential scattering coefficient has the form

$$\mu_s^i(\mathbf{r},\nu,\omega_s,t) = \mu_s^i(\mathbf{r},\nu,t)\overline{p}_i(\nu,\omega_s). \tag{51}$$

Finally, it is often assumed, for computational convenience, that scattering is isotropic. For this model, $\overline{p} = 1/(4\pi)$.

[2]Sometimes the phase function is normalized to $1/4\pi$. Such a phase function is denoted by Φ and is used by Siegel and Howell. I prefer the unit normalization since it has a direct probabilistic interpretation.

7 Radiative Transfer in Gases

7.1 Photoexcitation and Radiative Transitions

Radiation is absorbed or emitted from the atoms or molecules of a gas at discrete energies or *spectral lines*. Such line absorption or emission generally occurs over the whole spectrum of interest, and usually are the dominant absorption/emission processes in many radiative transfer problems. When a photon is absorbed, an orbital electron is excited from an energy level E_i to a higher energy level E_j. For such a photoexcitation reaction, the incident photon must have an energy very close to $h\nu_{ij} = E_j - E_i$. Equivalently, photons can be absorbed by a molecule to excite rotational or vibrational states which also have discrete energies.

The inverse of this absorption reaction also occurs, either spontaneously or by being induced by an incident photon of the same energy, so that the electron in the excited energy state E_j returns to the lower state E_i with a photon of energy $h\nu_{ij} = E_j - E_i$ being emitted. The decay of the excited state can also produce a cascade of lower energy photons as a result of the electron reaching E_i by way of intermediate energy states. Also non-radiative transitions can occur when the energy change is absorbed into other energy states of a molecule (e.g., rotational or vibrational states).

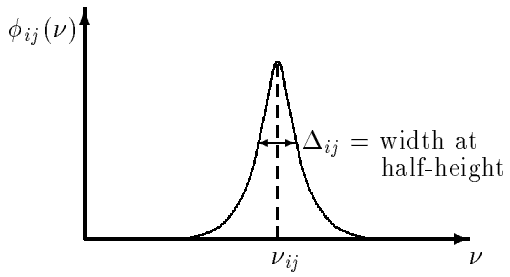

Figure 12. An absorption-line profile for transition between energy states E_i and E_j.

For a particular electronic transition ij, absorbed or emitted photons can have a small range of frequencies about the central frequency ν_{ij} as a result of the Heisenberg uncertainty principle. This principle states that the uncertainty or variation of photon energy $\Delta E \simeq \hbar/\Delta t$ where $\hbar = h/(2\pi)$ and Δt is the uncertainty or variation in the transition time. This variation in ΔE leads to the *natural* line profile $\phi_{ij}(\nu)$ (see Fig. 12). The line profile is normalized such that $\phi_{ij}(\nu)\, d\nu$ is the probability a photon in $d\nu$ about ν is absorbed (or emitted) for transition ij. The natural profile is usually well described by a Lorentz distribution

$$\phi_{ij}(\nu) = \frac{\Delta_{ij}}{\Delta_{ij}^2 + (\nu - \nu_{ij})^2}. \tag{52}$$

The natural line width is usually broadened (or even narrowed) as a result of medium interactions. The effects that modify the natural line shape include the following.

Doppler Broadening: If an atom moving towards an observer with a speed v emits a photon of frequency ν_{ij}, the photon frequency will be increased to $\nu = \nu_{ij}(1 + v/c)$. Similarly, if the atom moves away from the observer, the frequency decreases to $\nu = \nu_{ij}(1 - v/c)$. This Doppler effect causes the line profile to be broadened into a Maxwellian profile

$$\phi_{ij}(\nu) = \frac{1}{\Delta_D}\sqrt{\frac{\ln 2}{\pi}} \exp\left[-(\nu - \nu_{ij})^2 \frac{\ln 2}{\Delta_D^2}\right], \tag{53}$$

where Δ_D is the width at half maximum

Collision Broadening: As the pressure of a gas increases, the collision rate among the gas atoms and molecules increases. These collisions perturb the energy states of the atoms and cause

broadening of the spectral lines. The resulting line profile is a Lorentz distribution, Eq. (52), but with an increased half-width $\Delta_C > \Delta_{ij}$.

Collision Narrowing: As pressure increases and more atomic collisions occur in the medium, the thermal motion of the atoms is restricted and the Doppler effect is not as effective at broadening the line, i.e., the line profile appears to narrow.

Stark Broadening: For gases with strong electric fields, such as in ionized gases, the electric field can severely perturb the energy levels of the atoms and molecules, often leading to large amounts of line broadening.

Calculation of line profiles is a very complex task, well beyond the scope of these notes. We will simply assume that the profiles $\phi_{ij}(\nu)$ are known.

7.1.1 Contributions to Extinction and Emission Coefficients

(a) Spontaneous Emission: Radiation emitted spontaneously from an excited state is emitted isotropically. If there are $N_j(\mathbf{r}, t)$ atoms per unit volume at $\mathbf{r}$ at time t in excited energy state j, then the spontaneous emission rate of radiant energy, per steradian per unit volume, within unit frequency about ν, that leaves the atom in lower state i is given by

$$R_{ji}^{\text{spontaneous}} = \frac{1}{4\pi} N_j A_{ji} \phi_{ij}(\nu) h\nu_{ij}. \tag{54}$$

Here A_{ji} is the Einstein coefficient which characterizes the spontaneous decay rate of state j to state i.

(b) Line Absorption: The rate at which the incident intensity $I_\nu(\mathbf{r}, \mathbf{\Omega}, t)$ is absorbed, per unit volume, by atoms in state i and causes a transition to state j is

$$R_{ij}^{\text{line}} = \frac{1}{4\pi} N_i B_{ij} h\nu_{ij} \phi_{ij}(\nu) I_\nu, \tag{55}$$

where B_{ij} is the second Einstein coefficient, related to A_{ji} by $A_{ji} = B_{ij}[2h\nu_{ij}^3/c^2]$.

(c) Induced Absorption: The rate at which radiant energy is emitted, per unit volume per steradian per unit frequency, by incident radiation I_ν that induces a transition from state j to state i is

$$R_{ji}^{\text{induced}} = \frac{1}{4\pi} N_j B_{ij} h\nu_{ij} \phi_{ij}(\nu) I_\nu. \tag{56}$$

Note that the angular dependence of the induced photons is that of I_ν.

With these expressions, their contributions to the extinction and emission coefficients can be written explicitly. The corrected extinction coefficient has contributions from terms (b) and (c), i.e.,

$$\begin{aligned} \rho(\mathbf{r}, t)\kappa'_\nu(\mathbf{r}, t) &= \{R_{ij}^{\text{line}} - R_{ji}^{\text{induced}}\} \\ &= \frac{1}{4\pi}[N_i(\mathbf{r}, t) - N_j(\mathbf{r}, t)] B_{ij} \phi_{ij}(\nu) h\nu_{ij}. \end{aligned} \tag{57}$$

The corrected mass emission coefficient contribution's from spontaneous emission is obtained from (a) as

$$\rho(\mathbf{r}, t)\epsilon'_\nu(\mathbf{r}, t) = \frac{1}{4\pi} N_j(\mathbf{r}, t) A_{ji} \phi_{ij}(\nu) h\nu_{ij}. \tag{58}$$

In the above formulation, it has been assumed $\phi_{ij}(\nu)$ is the same for both absorption and emission for transitions between states i and j. This approximation is called "complete redistribution" and is usually quite a good assumption.

In Eq. (57), N_i is usually greater than N_j so that κ'_ν is positive and radiation is exponentially attenuated as it streams through a medium, i.e. $I_\nu(s) = I_\nu(0)\exp[-\kappa_\nu s]$. However, with a "population inversion," $N_j > N_i$, there is an exponential increase with penetration distance such as occurs in a laser.

The ratio of corrected to uncorrected extinction coefficients is found to be

$$\frac{\kappa'_\nu(ij)}{\kappa_\nu(ij)} = 1 - \frac{N_j}{N_i}. \tag{59}$$

If a condition known as "Local Thermodynamic Equilibrium" (LTE) exist at the point where the state densities are being considered, then

$$\frac{N_j}{N_i} \underset{\text{LTE}}{\longrightarrow} \exp\left[-\frac{h\nu_{ij}}{kT}\right] < 1. \tag{60}$$

Thus, under LTE conditions, a population inversion cannot occur.

7.1.2 Photoionization and Radiative Recombination

Another important class of photon interactions are bound-free processes in which a free electron combines with an ion and emits a photon or, inversely, a photon ionizes a neutral atom. The former process contributes to the emission coefficient, and the later to the extinction coefficient. These two reactions and their rates can be written as

$$h\nu + N_Z \longrightarrow N_{Z+1} + e \qquad \text{rate} = \alpha_Z N_Z I_\nu \tag{61}$$

$$e + N_{Z+1} \longrightarrow NZ + h\nu \qquad \text{rate} = \beta_{Z+1} N_{Z+1} N_e. \tag{62}$$

Here α and β are appropriate interaction and rate coefficients and N_e is the free electron density. For simplicity of notation, we denote the ion density N_Z as just another atomic/state density N_i.

7.1.3 Scattering

Photons can also be scattered by the atoms of a gas, most commonly as coherent elastic scatters in which negligible energy or frequency change occurs. Such scattering is often very important in dilute gases such as those in planetary atmospheres. Also, in optically thick media or in line self-absorption in which a photon can be absorbed and reemitted many times before it escapes or is destroyed by some nonradiative event is scattering important. For other gaseous media, scattering with significant change in energy can occur.

The scattering interaction coefficient μ_s^i from atoms in state i is proportional to the density N_i of such states, i.e.

$$\mu_s^i(\mathbf{r}, \nu' \to \nu, \mathbf{\Omega}\bullet\mathbf{\Omega}', t) = \sigma_s^i(\nu' \to \nu, \mathbf{\Omega}\bullet\mathbf{\Omega}')N_i(\mathbf{r}, t) \tag{63}$$

where the constant of proportionality σ_s^i is seen to have dimensions of area and is called the *microscopic scattering cross section.*

The rate at which photon energy is scattered from atoms in the ith state, per unit volume, into unit solid angle about $\mathbf{\Omega}$ and into unit frequency about ν is

$$R_{ji}^{\rm scat} = \int_0^\infty d\nu' \int_{4\pi} d\Omega' \, \sigma_s^i(\nu' \to \nu, \mathbf{\Omega}\bullet\mathbf{\Omega}') N_i(\mathbf{r},t) I_{\nu'}(\mathbf{r},\mathbf{\Omega}',t). \tag{64}$$

This scattered energy contributes to the emission coefficient. This differential scattering cross section can be written in terms of the phase function as

$$\sigma_s^i(\nu' \to \nu, \mathbf{\Omega}\bullet\mathbf{\Omega}') = \sigma_s^i(\nu) p_i(\nu' \to \nu, \mathbf{\Omega}\bullet\mathbf{\Omega}'). \tag{65}$$

7.2 Calculation of Extinction and Emission Coefficients for Gases

The above contributions to the extinction and emission coefficients are now combined to give an explicitly expressions for κ_ν' and ϵ_ν'. The corrected absorption coefficient becomes

$$\rho\kappa_\nu' I_\nu = \{[\text{line-absorption} - \text{induced-emission}] + \text{non-line abs.} + \text{scatter from } (\nu, \mathbf{\Omega})\}$$

$$= \frac{1}{4\pi} \sum_{\substack{i,j \\ E_i < E_j}} \phi_{ij}(\nu) h\nu_{ij} [N_i - N_j] B_{ij} I_\nu + \sum_i \alpha_i N_i I_\nu + \sum_i N_i \sigma_s^i I_\nu \tag{66}$$

where α_i is the absorption cross section for processes other than line absorption (bound-bound), such as photoionization (bound-free) or bremsstrahlung (free-free) reactions. Similarly, the corrected emission coefficient becomes

$$\rho\epsilon_\nu' = \{\text{spontaneous line emission} + \text{non-line emission} + \text{scattered photons}\}$$

$$= \frac{1}{4\pi} \sum_{\substack{i,j \\ E_i < E_j}} \phi_{ij}(\nu) h\nu_{ij} N_j A_{ji} + \sum_i \beta_i N_i N_e$$

$$+ \sum_i \int_0^\infty d\nu' \int_{4\pi} d\Omega' \, \sigma_s^i(\nu' \to \nu, \mathbf{\Omega}\bullet\mathbf{\Omega}') N_i(\mathbf{r},t) I_{\nu'}(\mathbf{r},\mathbf{\Omega}',t). \tag{67}$$

where β_i is the rate coefficient for non-line emission process such as radiative recombination.

To evaluate the extinction and emission coefficients from the above formulation, it is necessary to know the N_i, the density of states and species. The rate equations for these population densities have the form

$$\frac{\partial N_i(\mathbf{r},t)}{\partial t} + \nabla\bullet(N_i \mathbf{u}) = \sum_j W_{ij} N_j, \qquad i = 1, \ldots, n \tag{68}$$

where $\mathbf{u}(\mathbf{r},t)$ is the gas velocity. The rate coefficients W_{ij} involve more processes than just photon interactions. For example, electron collisions can cause states to change as in

$$\mathrm{e} + N_i \rightleftharpoons N_j + \mathrm{e} \qquad \text{excitation/deexcitation by free electron} \tag{69}$$

$$\mathrm{e} + N_Z \rightleftharpoons N_{Z+1} + \mathrm{e} + \mathrm{e} \qquad \text{electron ionization/3-body ionization} \tag{70}$$

The rate coefficients have the form

$$W_i j = N_i R_{ij} - N_j R_{ji} \tag{71}$$

where R_{ij} is the probability, per unit differential time, that state/species i is transformed to state/species j and has the form

$$R_{ij} = A_{ij} + B_{ij}\frac{1}{4\pi}\int_0^\infty d\nu \left[\int_{4\pi} d\Omega\, I_\nu(\mathbf{r},\mathbf{\Omega},t)\right]\phi_{ij}(\nu) + C_{ij}\overline{v}_e N_e(\mathbf{r},t). \tag{72}$$

where the first term arises from spontaneous deexcitation, the second from photon line absorption, and the last term from electron collisions. To complete the set of equations, an equation analogous to Eq. (68) must be used to describe $N_e(\mathbf{r},t)$. For steady-state problems, the rate coefficients $W_{ij} \longrightarrow 0$, and the steady-state densities N_i can be found directly from Eq. (71).

From the above description, it is seen that calculation of the extinctions and emission coefficients is generally a very complex problem, requiring the calculation of many population densities for the myriad of energy states and species that can occur in hot gases. Fortunately, there is a very significant simplification if the medium can be assumed to be in *local thermodynamic equilibrium.* This is discussed next section.

It is seen from the above formulation, that the corrected emission coefficient has two components: the secondary scattered radiation and the spontaneously emitted radiation. It is the anisotropically scattered radiation which makes ϵ'_ν a function of the photon direction $\mathbf{\Omega}$; the spontaneous emission of radiation is generally isotropic. To separate these two contributions, we write $\epsilon'_\nu(\mathbf{r},\mathbf{\Omega},t) = \epsilon'^e_\nu(\mathbf{r},t) + \epsilon'^s_\nu(\mathbf{r},\mathbf{\Omega},t)$. The scattered contribution can be expressed in terms of the differential scattering coefficient by summing Eqs. (63) and (64) over all species/state i. With this explicit separation of the scattered radiation from the spontaneously emitted radiation, the RTE, Eq. (41), can be written as

$$\left[\frac{1}{c}\frac{\partial}{\partial t} + \mathbf{\Omega}\bullet\mathbf{\nabla}\right] I_\nu(\mathbf{r},\mathbf{\Omega},t) = -\rho(\mathbf{r},t)\kappa'_\nu(\mathbf{r},t)I_\nu(\mathbf{r},\mathbf{\Omega},t) + \rho(\mathbf{r},t)\epsilon'^e_\nu(\mathbf{r},t)$$
$$+ \int_0^\infty d\nu' \int_{4\pi} d\Omega'\, \mu_s(\mathbf{r},\nu'\to\nu,\mathbf{\Omega}\bullet\mathbf{\Omega}')I_{\nu'}(\mathbf{r},\mathbf{\Omega}',t). \tag{73}$$

7.3 Local Thermodynamic Equilibrium

Under the assumption of *local thermodynamic equilibrium* (LTE), it is assumed that the radiation field is sufficiently dilute so ionization and excitation produced by electron/atom collisions far exceeds that from photon interactions. Thus, LTE is maintained solely by electron/atom collisions. Under LTE, *all* pairs of state densities of the same atom are related by the so-called Boltzmann factor

$$\frac{N_j}{N_i} \underset{\text{LTE}}{\longrightarrow} \frac{g_j}{g_i}\exp\left[-\frac{h\nu_{ij}}{kT}\right] \tag{74}$$

where g_i is a *statistical weight factor* and k is Boltzmann's constant. From this result we see that for $E_j > E_i$, $N_j < N_i$ (with $g_i \simeq g_j$), and population inversions cannot occur. From this relation, the population densities N_i can be found rather than from the much more complex set of equations of Eq. (68).

However, a more important consequence of LTE is that photon emission becomes a smooth function of frequency no matter how complex the line structure. In steady-state and at a point where there is LTE at a temperature T, the photon energy being absorbed must equal the energy emitted in any direction and frequency, i.e.,

$$\mu_a(\mathbf{r})I_\nu(\mathbf{r},\mathbf{\Omega}) = \rho(\mathbf{r})\epsilon'^e_\nu(\mathbf{r}). \tag{75}$$

However, the spectral intensity for such a medium is just Planck's black-body spectrum $B_\nu(T)$. Thus under LTE

$$\rho\epsilon'^{e}_{\nu}(\mathbf{r}) \underset{\text{LTE}}{\longrightarrow} \mu_a B_\nu(T(\mathbf{r})) = \mu_a \frac{2h\nu^3/c^2}{e^{h\nu/kT}-1}. \tag{76}$$

This consequence of LTE is sometime called Kirchhoff's law, and represents an enormous simplification! ϵ'^{e}_{ν} is now a smooth function (no emission lines) determined by a single parameter T.

For the time-dependent case, as we have assumed throughout our discussion, LTE still applies if the time dependence of the radiation field (i.e, of $I_\nu(\mathbf{r},\mathbf{\Omega},t)$) is determined by a relatively slow temporal variation of radiation sources or boundary conditions. In other words, when the time required for the atoms of a medium to come into LTE with the radiation field is much less than the time for $I_\nu(\mathbf{r},\mathbf{\Omega},t)$ to change appreciably, Eq. (76) still is valid.

Although ϵ'^{e}_{ν} is tremendously simplified under an LTE assumption , the extinction coefficient κ'_ν is still complicated. The population densities N_i needed for κ'_ν, however, are now much easier to determine since they are now known in terms of the local temperature T and density ρ.

Note, LTE says nothing about the radiation field I_ν. It is often mistakenly thought that LTE implies that $I_\nu = B_\nu$. Only in an infinite isothermal medium does the solution of the LTE-RTE yield $I_\nu = B_\nu$, so that LTE is self-consistent (see Section 8.2. Generally, however, this is not the case.

As a final observation, LTE is not necessarily even a good approximation. For example, it does not hold in stellar atmospheres where atom densities are low and atomic collisions do not dominate. However, LTE is almost always assumed (even when not rigorously valid) since, without it, the RTE would be intractable.

7.4 The Steady-State RTE with LTE and Elastic Scattering

In almost all radiative transfer situations, the radiation field does not change in time or it varies slowly (compared to the time required for photons to move through the region of interest) as a result of, for example, sources changing in time (such as the sun moving across the sky). Even if the sources, medium properties, and/or boundary conditions change in time, the radiation field relaxes nearly instantly to a steady distribution determined by the medium and source properties. The radiation field is thus always in quasi-steady state with the instantaneous medium and source properties.

In the transport of thermal radiation, inelastic scattering processes (e.g., Compton and Raman scattering) are usually negligible and only elastic scattering need be considered. For elastic scattering there is negligible change in frequency between the incident and scattered radiation. For such scattering in an isotropic medium

$$\mu_s(\mathbf{r},\nu' \to \nu, \mathbf{\Omega}\bullet\mathbf{\Omega}') \longrightarrow \mu_s(\mathbf{r},\nu)\overline{p}(\mathbf{r},\nu,\mathbf{\Omega}\bullet\mathbf{\Omega}')\delta(\nu-\nu'). \tag{77}$$

Substitution of this result into Eq. (73), use of the steady-state assumption, and recognition that $\rho\kappa'_\nu = \mu_a + \mu_s$ allows the RTE to be written as

$$\mathbf{\Omega}\bullet\nabla I_\nu(\mathbf{r},\mathbf{\Omega}) + \rho(\mathbf{r})\kappa'_\nu(\mathbf{r})I_\nu(\mathbf{r},\mathbf{\Omega}) = \rho(\mathbf{r})\kappa'_\nu(\mathbf{r})\Big[\gamma_\nu B_\nu(T) + (1-\gamma_\nu)\int_{4\pi} d\Omega'\,\overline{p}(\mathbf{r},\nu,\mathbf{\Omega}\bullet\mathbf{\Omega}')I_\nu(\mathbf{r},\mathbf{\Omega}')\Big] \tag{78}$$

where $\gamma_\nu \equiv \mu_a/(\mu_a + \mu_s)$, the ratio of the corrected capture (absorption minus induced) to total (capture plus scatter) cross sections.

With these approximations, the RTE becomes monochromatic, i.e., photons of one frequency interact independently of photons of other frequencies. By far, most of the theoretical work on radiative transfer has been based on this form of the RTE, since, with it, I_ν can be obtained as a series of independent monochromatic calculations.

7.4.1 Isotropic Scattering

For simplicity, scattering is often assumed to be isotropic, i.e. $\overline{p}(\mathbf{r}, \nu, \mathbf{\Omega}\bullet\mathbf{\Omega}') = 1/(4\pi)$. This is a terrible assumption for scattering from aerosols and dust particles (described by Mie scattering) but less so for scattering from atoms. In any event, if isotropic scattering is appropriate, Eq. (78) reduces to

$$\mathbf{\Omega}\bullet\nabla I_\nu(\mathbf{r}, \mathbf{\Omega}) + \rho(\mathbf{r})\kappa'_\nu(\mathbf{r})I_\nu(\mathbf{r}, \mathbf{\Omega}) = \rho(\mathbf{r})\kappa'_\nu(\mathbf{r})\left[\gamma_\nu B_\nu + (1-\gamma_\nu)J_\nu(\mathbf{r})\right] \tag{79}$$

where the *average intensity* is defined as

$$J_\nu(\mathbf{r}) \equiv \frac{1}{4\pi}\int_{4\pi} d\Omega\, I_\nu(\mathbf{r}, \mathbf{\Omega}). \tag{80}$$

Two limiting cases of this form of the RTE are widely studied. First, if the capture processes are small compared to scattering, $\gamma_\nu \to 0$. Such an approximation is often used in planetary atmosphere calculations in which absorptions are few compared to scatters. At the other extreme, one can ignore scattering if the atom density becomes sufficiently high, as often is the case in astrophysical calculations involving dense media. Under this approximation, $\gamma_\nu \to 1$ so the RTE becomes

$$\mathbf{\Omega}\bullet\nabla I_\nu(\mathbf{r}, \mathbf{\Omega}, t) + \rho(\mathbf{r})\kappa'_\nu(\mathbf{r})I_\nu(\mathbf{r}, \mathbf{\Omega}) = \rho(\mathbf{r})\kappa'_\nu(\mathbf{r})B_\nu(T). \tag{81}$$

If the temperature profile $T(\mathbf{r})$ is known, this result can be integrated directly to give $I_\nu(\mathbf{r}, \mathbf{\Omega})$.

7.4.2 Grey Approximation

Under the grey approximation γ_ν, κ'_ν, and $\overline{p}(\mathbf{r}, \nu, \mathbf{\Omega}\bullet\mathbf{\Omega}')$ are assumed to be independent of ν (or replaced by some appropriate average over the frequencies of interest). Thus if γ_ν and κ'_ν are constants and for a frequency-independent phase function, then integration of Eq. (78) over all frequencies yields

$$\begin{aligned}\mathbf{\Omega}\bullet\nabla I(\mathbf{r}, \mathbf{\Omega}) + \rho\kappa' I(\mathbf{r}, \mathbf{\Omega}) &= \rho\kappa'\left[\gamma\int_0^\infty d\nu\, B_\nu(T) + (1-\gamma)\int_{4\pi} d\Omega'\,\overline{p}(\mathbf{r}, \mathbf{\Omega}\bullet\mathbf{\Omega}')I(\mathbf{r}, \mathbf{\Omega}')\right] \\ &= \rho\kappa'\left[\gamma\frac{\sigma}{\pi}T^4 + (1-\gamma)\int_{4\pi} d\Omega'\,\overline{p}(\mathbf{r}, \mathbf{\Omega}\bullet\mathbf{\Omega}')I(\mathbf{r}, \mathbf{\Omega}')\right]\end{aligned} \tag{82}$$

where the total intensity $I(\mathbf{r}, \mathbf{\Omega}) = \int_0^\infty d\nu\, I_\nu(\mathbf{r}, \mathbf{\Omega})$. Thus, the calculation of the total radiation intensity becomes independent of frequency, i.e., a single monochromatic calculation is all that is needed.

Three averages of κ'_ν are widely used for LTE problems [Stewart, 1967]:

Rosseland Average:

$$\kappa_R \equiv \int_0^\infty d\nu\,\frac{\partial B_\nu(T)}{\partial T}\Big/\int_0^\infty d\nu\,\frac{1}{\kappa'_\nu}\frac{\partial B_\nu(T)}{\partial T} \tag{83}$$

Planck Average:

$$\kappa_P \equiv \int_0^\infty d\nu\, \kappa'_\nu B_\nu(T) \Big/ \int_0^\infty d\nu\, B_\nu(T) \tag{84}$$

Transmission Mean:

$$\kappa_T(m) \equiv -\frac{1}{m} \ln \left[\int_0^\infty d\nu\, e^{-m\kappa'_\nu} B_\nu(T) \Big/ \int_0^\infty d\nu\, B_\nu(T) \right]. \tag{85}$$

Such spectrum averages are called *mean opacities* or simply *opacities* (a complicated usage since κ'_ν is also often called a opacity). The above three average opacities are applicable to calculation of frequency-integrated intensities in optically thick, optically thin, and isothermal regions, respectively.

7.4.3 Uniform Picket Fence Model

A extension of the grey approximation is to assume the optical properties are constant (or averaged) over G contiguous frequency ranges (or *groups*) $\Delta\nu_g$, $g = 1, \ldots, G$ covering the entire frequency spectrum. Integration of Eq. (78) over $\Delta\nu_g$ gives the monochromatic RTE equation

$$\boldsymbol{\Omega}\bullet\boldsymbol{\nabla} I_g(\mathbf{r},\boldsymbol{\Omega}) + \rho(\mathbf{r})\kappa'_g(\mathbf{r}) I_g(\mathbf{r},\boldsymbol{\Omega}) = \mu_{ag}(\mathbf{r}) B_g(T) + \mu_{sg}(\mathbf{r}) \int_{4\pi} d\Omega'\, \overline{p}_g(\mathbf{r}, \boldsymbol{\Omega}\bullet\boldsymbol{\Omega}') I_g(\mathbf{r},\boldsymbol{\Omega}'), \quad g = 1, \ldots, G. \tag{86}$$

The group optical constants are defined as follows:

$$I_g(\mathbf{r},\boldsymbol{\Omega}) = \int_{\Delta\nu_g} d\nu\, I_\nu(\mathbf{r},\boldsymbol{\Omega}), \tag{87}$$

$$\kappa_g(\mathbf{r}) = \frac{1}{I_g(\mathbf{r},\boldsymbol{\Omega})} \int_{\Delta\nu_g} d\nu\, \kappa_\nu(\mathbf{r}) I_\nu(\mathbf{r},\boldsymbol{\Omega}), \tag{88}$$

$$\mu_{ag}(\mathbf{r}) B_g(T) = \int_{\Delta\nu_g} d\nu\, \mu_a(\mathbf{r},\nu) B_\nu(T), \tag{89}$$

and

$$\mu_{sg}(\mathbf{r})\overline{p}_g(\mathbf{r},\boldsymbol{\Omega}\bullet\boldsymbol{\Omega}') = \frac{1}{I_g(\mathbf{r},\boldsymbol{\Omega})} \int_{\Delta\nu_g} d\nu\, \overline{p}(\mathbf{r},\nu,\boldsymbol{\Omega}\bullet\boldsymbol{\Omega}') I_\nu(\mathbf{r},\boldsymbol{\Omega}). \tag{90}$$

The above picket fence model (or multigroup) approximation is exact provided the group optical constants can be evaluated exactly, for which $I_\nu(\mathbf{r},\boldsymbol{\Omega})$ must first be known. However, if within each $\Delta\nu_g$ intervals, $I_\nu(\mathbf{r},\boldsymbol{\Omega})$ can be approximated by a constant, the group constants can be estimated without first knowing $I_\nu(\mathbf{r},\boldsymbol{\Omega})$. The group intensities I_g can then be solved from Eq. (86) as a series of independent monochromatic RTE problems. Finally, it should be observed that the grey approximation is just the picket fence model with a single frequency interval $(0,\infty)$.

7.4.4 Plane Geometry with Azimuthal Symmetry

In many radiative transfer situations, the geometry can be approximated by one-dimensional plane geometry, i.e., the radiation intensity depends on only one spatial dimension x (say) so that $I_\nu(\mathbf{r},\boldsymbol{\Omega}) \longrightarrow I_\nu(x,\boldsymbol{\Omega}) = I_\nu(x,\theta,\psi) = I_\nu(x,\omega,\psi)$ where $\omega = \cos\theta$. For example, radiative transfer in planetary or stellar atmospheres, penetration of light into sea water, and coal-dust combustion

confined by plane parallel walls are all well described by a one-dimensional plane geometry. In such a geometry, Eq. (78) becomes

$$\omega\frac{\partial I_\nu(x,\omega,\psi)}{\partial x}+\mu_e(x,\nu)I_\nu(x,\omega,\psi)=\mu_a(x,\nu)B_\nu(T)+$$
$$\mu_s(x,\nu)\int_0^{2\pi}d\psi'\int_{-1}^{1}d\omega'\,\overline{p}(x,\nu,\mathbf{\Omega}\bullet\mathbf{\Omega}')I_\nu(x,\omega',\psi') \quad (91)$$

where, for consistency of notation, the linear extinction coefficient $K_\nu=\rho(\mathbf{r})\kappa'_\nu(\mathbf{r})$ is now denoted as $\mu_e(x,\nu)=\mu_a+\mu_s$.

In many plane geometry problems, the intensity depends only weakly on the azimuthal angle, or, equivalently, one is interested in the azimuthally averaged intensity, i.e.,

$$\widehat{I}_\nu(x,\omega)\equiv\frac{1}{2\pi}\int_0^{2\pi}d\psi\,I_\nu(x,\omega,\psi). \quad (92)$$

Integration of Eq. (91) over ψ and division by 2π gives the following plane-geometry, azimuthally-symmetric form of the RTE:

$$\omega\frac{\partial\widehat{I}_\nu(x,\omega)}{\partial x}+\mu_e(x,\nu)\widehat{I}_\nu(x,\omega)=\mu_a(x,\nu)B_\nu(T)$$
$$+\mu_s(x,\nu)\int_{-1}^{1}d\omega'\,\widehat{p}(x,\nu,\omega'\rightarrow\omega)\widehat{I}_\nu(x,\omega') \quad (93)$$

where the azimuthally integrated phase function is defined as

$$\widehat{p}(x,\nu,\omega'\rightarrow\omega)\equiv\int_0^{2\pi}d\psi\,\overline{p}(x,\nu,\mathbf{\Omega}\bullet\mathbf{\Omega}'). \quad (94)$$

Since $\mathbf{\Omega}\bullet\mathbf{\Omega}'=\omega\omega'+\sqrt{1-\omega^2}\sqrt{1-\omega'^2}\cos(\psi-\psi')$, the integration over ψ in the right-hand side of Eq. (94) also eliminates the ψ' dependence, so that $\widehat{p}$ depends only on the ω and ω' angular variables.

This form of the RTE forms the basis for the remainder of our discussion in these notes. The RTE with LTE and elastic scattering is a monochromatic equation in which the intensity at one frequency is independent of the intensity at another.

7.4.5 Boundary Conditions

To determine a unique solution of Eq. (93), it is necessary to specify the incident radiation intensity at the surfaces of the medium, i.e., at $x=0$ and at $x=X$. The simplest boundary conditions are to specify the radiation emitted by the bounding surfaces into the medium. Thus

$$I_\nu(0,\omega)=f(\nu,\omega), \qquad \text{for } \omega>0, \quad (95)$$

$$I_\nu(X,\omega)=g(\nu,\omega), \qquad \text{for } \omega<0, \quad (96)$$

where $f(\nu,\omega)$ and $g(\nu,\omega)$ are the prescribed incident intensities from the walls into the medium. These incident intensities for physical solid bounding walls are determined by the wall emissions which generally vary as the fourth power the wall temperature.

If, in addition to a specified incident intensity at a boundary, a fraction of the outgoing radiation is diffusely reflected back into the medium, the boundary conditions become

$$I_\nu(0,\omega) = f(\nu,\omega) - 2\alpha_1(\nu)\int_{-1}^{0} d\omega\,\omega I_\nu(0,\omega), \qquad \text{for } \omega > 0, \tag{97}$$

$$I_\nu(X,\omega) = g(\nu,\omega) + 2\alpha_2(\nu)\int_{0}^{1} d\omega\,\omega I_\nu(X,\omega), \qquad \text{for } \omega < 0, \tag{98}$$

where α_1 and α_2 are the reflectivities of the bounding surfaces at $x = 0$ and $x = X$, respectively.

8 Equilibrium Models

The RTE discussed above contain the emission term $\mu_a B_\nu(T)$ which depends on the temperature profile $T(\mathbf{r})$. If $T(\mathbf{r})$ is known *a priori*, then (numerical) solution of the RTE gives the radiation field $I_\nu(\mathbf{r},\mathbf{\Omega})$. However, $T(\mathbf{r})$ generally is unknown and depends very non-linearly on the radiation field. Thus, some other assumption, besides LTE, is needed. The most common additional assumption is that the local radiation field is in equilibrium with the local emission of radiant energy. This is discussed next.

8.1 Local Radiative Equilibrium

Under local radiation equilibrium, the radiant energy absorbed at any point in the medium equals that emitted. Mathematically,

$$\int_0^\infty d\nu\,\mu_a(\mathbf{r},\nu)\int_{4\pi} d\Omega\; I_\nu(\mathbf{r},\mathbf{\Omega}) = \int_0^\infty d\nu\int_{4\pi} d\Omega\;\rho(\mathbf{r})\epsilon'_\nu(\mathbf{r},\mathbf{\Omega}). \tag{99}$$

If, in addition, LTE applies, radiative equilibrium requires

$$\int_0^\infty d\nu\,\mu_a(\mathbf{r},\nu)\int_{4\pi} d\Omega\; I_\nu(\mathbf{r},\mathbf{\Omega}) = 4\pi\int_0^\infty d\nu\,\mu_a(\mathbf{r},\nu)B_\nu[T(\mathbf{r})]. \tag{100}$$

If there are other sources of thermal energy (e.g., chemical reactions, heat conduction contributions, and/or convective flow of heat), such that $S_{ex}(\mathbf{r})$ is the rate at which thermal energy is transferred to the medium per unit volume by non-radiative processes, the radiation equilibrium condition becomes

$$\int_0^\infty d\nu\,\mu_a(\mathbf{r},\nu)\int_{4\pi} d\Omega\; I_\nu(\mathbf{r},\mathbf{\Omega}) + S_{ex}(\mathbf{r}) = 4\pi\int_0^\infty d\nu\,\mu_a(\mathbf{r},\nu)B_\nu[T(\mathbf{r})]. \tag{101}$$

Under a grey approximation μ_a is independent of ν, and Eq. (101) reduces to

$$\mu_a(\mathbf{r})\int_0^\infty d\nu\int_{4\pi} d\Omega\; I_\nu(\mathbf{r},\mathbf{\Omega}) + S_{ex}(\mathbf{r}) = 4\pi\mu_a(\mathbf{r})\int_0^\infty d\nu\, B_\nu[T(\mathbf{r})] = 4\mu_a(\mathbf{r})\sigma T^4(\mathbf{r}), \tag{102}$$

where σ is the Stephan-Boltzmann constant. It is Eq. (101) or (102) that relates the temperature distribution in a medium to the radiation field.

For radiation transport problems in which $T(\mathbf{r})$ is unknown, The RTE must be solved subject to the constraint of Eqs. (100), (101), or (102). This requirement suggests an iterative solution scheme. First, guess a temperature profile and then solve the RTE for I_ν. Next revise the estimate of $T(\mathbf{r})$ from the radiation equilibrium condition (i.e. solve Eq. (102) for T($\mathbf{r}$)). Continue in this fashion by repetitively solving the RTE and revising $T(\mathbf{r})$ from the local radiative equilibrium condition until convergence is achieved.

8.2 Global Radiation Equilibrium

In an infinite, homogeneous, isothermal medium, in which radiation is in equilibrium with the surroundings, the radiation intensity cannot depend on position $\mathbf{r}$, direction $\mathbf{\Omega}$, or time t. In this situation $I_\nu(\mathbf{r},\mathbf{\Omega},t) \longrightarrow I_\nu^o$, a constant, and Eq. (78) becomes

$$\left[\frac{1}{c}\frac{\partial}{\partial t} + \mathbf{\Omega}\bullet\mathbf{\nabla}\right] I_\nu^o = \rho\kappa_\nu'(\mathbf{r},t)\left[-I_\nu^o + \gamma_\nu B_\nu + (1-\gamma_\nu)I_\nu^o \int_{4\pi} d\Omega'\,\overline{p}(\nu,\mathbf{\Omega}\bullet\mathbf{\Omega}')\right]. \tag{103}$$

Because I_ν^o is a constant, the left-hand side of the above equation equals zero, and since $\int_{4\pi} d\Omega'\,\overline{p}(\nu,\mathbf{\Omega}\bullet\mathbf{\Omega}') = 1$, this equation immediately reduces to

$$I_\nu^o = B_\nu(T), \tag{104}$$

i.e., the spectral intensity becomes that of Planck's black-body spectrum. For this special case the radiation field has the following properties:

energy density:

$$u_\nu^o = \frac{1}{c}\int_{4\pi} d\Omega\; I_\nu^o = \frac{4\pi}{c}B_\nu(T) \tag{105}$$

total energy density:

$$u^o = \int_0^\infty d\nu\; u_\nu^o = \frac{4}{c}\sigma T^4 \tag{106}$$

radiant heat flux vector:

$$\mathbf{q}^o = \mathbf{0} \tag{107}$$

radiation pressure tensor:

$$P_{ij}^o = \frac{4}{3c}\sigma T^4\delta_{ij} \tag{108}$$

9 Numerical Methods for Solving the RTE

In this section, several numerical methods are presented for solving the RTE with elastic scattering and azimuthal symmetry in plane geometry. To simplify notation, the $\widehat{\ }$ accents are dropped, so Eq. (93) is written as

$$\left[\omega\frac{\partial}{\partial x} + \mu_e(\nu,x)\right] I_\nu(x,\omega) = \mu_s(\nu,x)\int_{-1}^{1} d\omega'\,p(\nu,x,\omega'\to\omega)I_\nu(x,\omega') + \mu_a(\nu,x)B_\nu(T). \tag{109}$$

As another notational simplification, we measure distance in terms of optical thickness $\tau(x) \equiv \int_0^x dx'\,\mu_e(x')$ so that $d\tau = \mu_e\,dx$. Thus the above RTE can be written as

$$\omega\frac{\partial I_\nu(\tau,\omega)}{\partial\tau} + I_\nu(\tau,\omega) = \gamma_s(\nu,\tau)\int_{-1}^{1} d\omega'\,p(\nu,x,\omega'\to\omega)I_\nu(x,\omega') + \gamma_a(\nu,\tau)B_\nu(T). \tag{110}$$

where the *single-scatter albedo* $\gamma_s \equiv \mu_s/\mu_e$ and $\gamma_a(\tau) \equiv \mu_a/\mu_e$. The slab boundaries are at $x = 0$ and at $x = X$, or at optical depths $\tau = 0$ and $\tau = \xi$. The boundary conditions are given by Eqs. (97) and (98).

If the medium is assumed grey (i.e., γ_s, γ_a, and p are independent of ν), integration of Eq. (110) over all frequencies yields following equation for the total intensity $I(\tau,\omega) = \int_0^\infty d\nu\, I_\nu(\tau,\omega)$

$$\omega\frac{\partial I(\tau,\omega)}{\partial\tau} + I(\tau,\omega) = \gamma_s(\tau)\int_{-1}^{1} d\omega'\, p(x,\omega'\to\omega)I(x,\omega') + \gamma_a(\tau)\frac{\sigma T^4(T)}{\pi}, \tag{111}$$

in which the emission term is written explicitly in terms of the temperature.

Generally, the emission term $\gamma_a(\nu)B_\nu[T(x)]$ emission term generally depends very non-linearly on the temperature profile $T(x)$, which is usually not known *a priori*. The temperature profile is related to the radiation field through the local radiative equilibrium relation of Eq. (102) in which the thermal power generation term $S_{ex}(x)$ may also depend on the local temperature (e.g., in a chemically reacting medium). For a grey, plane-geometry medium, the local radiative equilibrium condition becomes

$$2\pi\mu_a(\tau)\int_{-1}^{1} d\omega\, I(\tau,\omega) + S_{ex}(\tau,T) = 4\mu_a(\tau)\sigma T^4(\tau). \tag{112}$$

To evaluate $T(\tau)$ from this equation, $I(\tau,\omega)$ is found from Eq. (111) by solving for the intensity $I(\tau,\omega)$ based on some assumed temperature profile. Then a revised temperature profile is obtained from Eq. (112). A new radiation field is then calculations, and such an iterative procedure (calculate $I(\tau,\omega)$, revise $T(\tau)$, revise $I(\tau,\omega)$...) is continued until convergence. For a non-grey medium, Eq. (110) must be solved for a series of frequencies and the more general local radiative condition of Eq. (101) must be used to revise $T(\tau)$.

Key to any radiative transfer problem is the solution of the RTE. Many methods have been developed. In the following subsections, three widely used techniques are discussed. To simplify notation in the subsequent sections, the variable ν in Eq. (110) is omitted: however, it should be remembered that I_ν, μ_e, μ_a, μ_s, B, and $\hat{p}$ are, in general, frequency dependent. Thus we consider the RTE in the form

$$\boxed{\omega\frac{\partial I(\tau,\omega)}{\partial\tau} + I(\tau,\omega) = \gamma_s(\tau)\int_{-1}^{1} d\omega'\, p(x,\omega'\to\omega)I(x,\omega') + \gamma_a(\tau)B(T).} \tag{113}$$

9.1 Discrete-Ordinates Method

The *discrete-ordinates method* is a name given to several closely related techniques for obtaining approximate solutions to the RTE. The principal feature in all these methods is the discretization of the angular variable $\mathbf{\Omega}$ such that photons are represented as streaming along only a finite number of directions $\mathbf{\Omega}_i$ rather than in all possible directions as allowed by the RTE. In the most modern and powerful of the discrete-ordinates techniques, the spatial variables are also discretized and numerical methods are used to obtain the angular radiation intensity at all the spatial and angular mesh points [Duderstadt and Martin 1979; Lewis and Miller 1984].

To illustrate the basic ideas of this powerful method, the discrete-ordinates technique is presented here for the simplest case of one-dimensional plane geometry with azimuthal symmetry (i.e., the RTE of Eq. (113)). The same ideas are applicable to other geometries, even with more than one spatial dimension; however, these extensions become algebraically much more complicated without introducing any additional principles of the discrete-ordinates method.

The azimuthally-averaged intensity for a given frequency in a slab of optical thickness ξ is given by Eq. (113). To obtain a unique solution, the incident intensity at the slab surfaces, $I(0,\omega)$ for $\omega > 0$, and $I(\xi,\omega)$ for $\omega < 0$ is specified by boundary conditions of Eqs. (97) and (98).

The first step in the discrete-ordinates method is to select a finite set of directions $\{\omega_i\}$, $i = 1, \ldots, N$, and a set of corresponding quadrature weights $\{w_i\}$, $i = 1, \ldots, N$, such that the scattering integral in Eq. (113) may be approximated by numerical integration (quadrature) as

$$\int_{-1}^{1} d\omega' \, p(\tau, \omega' \to \omega) I(\tau, \omega') \simeq \sum_{i=1}^{N} w_i \, p(\tau, \omega_i \to \omega) I(\tau, \omega_i). \tag{114}$$

The particular choice of the sets $\{\omega_i\}$ and $\{w_i\}$ depends on how accurately the radiation intensity is to be integrated by the quadrature approximation in Eq. (114). If there is some reason to believe that $I(x, \omega)$ has some special feature (e.g., the photons are mostly moving in some narrow range of ω), then a special choice of quadrature ordinates and weights may be indicated. However, in most cases no prior knowledge about the radiation intensity is available, and usually one chooses the ω_i's and w_i's based on a Gaussian quadrature approximation, in which the ω_i's are the N zeros of the Nth Legendre polynomial $P_N(\omega_i) = 0$ and the corresponding quadrature weights are given by

$$w_i = \frac{2(1 - \omega_i)^2}{[(N+1) P_{N+1}(\omega_i)]^2}. \tag{115}$$

This choice of $\{\omega_i\}$ and $\{w_i\}$ has the remarkable property that the scattering integral approximation of Eq. (114) is exact if $p(\tau, \omega' \to \omega)(\tau, \omega')$ is a polynomial in ω' of degree $(2N - 1)$ or less. No higher-degree polynomial can be integrated exactly by any N-point quadrature procedure. Thus, the choice of a Gaussian quadrature for Eq. (114) is optimum *for polynomials*. Although I and p are generally not polynomials, Gaussian quadrature is generally used since the radiation intensity and the phase function can be represented accurately by polynomials of sufficiently high degree. Finally, the quadrature order N is always taken as even to avoid an ordinate at $\omega = 0$, a direction at which $I(\tau, \omega)$ is discontinuous at the boundaries.

The next step in the discrete-ordinates method is to obtain a set of N equations for $I_i(\tau) \equiv I(\tau, \omega_i)$. Such equations can be obtained from the RTE, Eq. (113), in a number of ways, thus giving rise to different discrete-ordinates formulations [Case and Zweifel 1967]. For instance, Eq. (113) may be integrated over N angular subintervals (e.g., ω_{i-1} to ω_i, $i = 1, \ldots, N$) and a variety of approximations can be used to express these ω integrals in terms of the $I(\tau, \omega)$ (such as a linear variation in ω between the ω_i ordinates). However, for the present plane-geometry case, the required N equations for the $I(\tau)$ can be obtained directly by simply evaluating Eq. (113) at each ω_i, namely,[3]

$$\boxed{\omega_i \frac{\partial I_i(\tau)}{\partial \tau} + I_i(\tau) = Q_i(\tau), \quad i = 1, \ldots, N,} \tag{116}$$

where the total source Q_i is approximated as

$$Q_i(\tau) \simeq \gamma_s \sum_{j=1}^{N} w_j p(\tau, \omega_j \to \omega_i) I_j(\tau) + \gamma_a B(T). \tag{117}$$

These N equations are the discrete-ordinates equations which must be solved for $I_i(\tau)$.

[3] This procedure is equivalent to integrating the RTE over a small ω subinterval whose central point is ω_i. These ω integrals are then approximated by the product of the interval width and the integrand evaluated at the interval midpoint ω_i.

9.1.1 Numerical Solution of the Discrete-Ordinates Equations

For simple cases, the discrete-ordinates equations, Eqs. (116), may be solved directly in a semi-analytical manner. This was the procedure used in the original development of the discrete-ordinates method by Wick and Chandrasekhar [Chandrasekhar 1960]. However, this method is notoriously unstable numerically if $N \geq 8$ and is seldom used.

The most widely used method for solving the discrete-ordinates equations of Eq. (116) is to discretize the spatial variable and reduce the discrete-ordinates equations to a set of algebraic equations which gives the intensities only at the spatial and angular nodes. For the present case, divide the slab into K intervals by a mesh $\{\tau_k\}$, where $\tau_0 = 0$ and $\tau_K = T$. Integration of Eq. (116) over the kth spatial interval (τ_k, τ_{k+1}) gives

$$\omega_i[I_i(\tau_{k+1}) - I_i(\tau_k)] + \int_{\tau_k}^{\tau_{k+1}} I_i(\tau)\,d\tau = \int_{\tau_k}^{\tau_{k+1}} Q_i(\tau)\,d\tau,$$

$$i = 1, \ldots, N, \quad k = 0, 1, \ldots, K-1. \tag{118}$$

To evaluate the integrals in this result, it is assumed that the mesh width $\Delta\tau_k \equiv \tau_{k+1} - \tau_k$ is sufficiently small that the integrals can be approximated by their value at the mesh cell midpoints $\tau_{k+1/2} \equiv (\tau_{k+1} + \tau_k)/2$. Thus, Eq. (118) is approximated as

$$\omega_i \frac{I_i(\tau_{k+1}) - I_i(\tau_k)}{\Delta\tau_k} + I_i(\tau_{k+1/2}) \simeq Q_i(\tau_{k+1/2}). \tag{119}$$

This finite-difference equation relates the value of the radiation intensity at the mesh cell boundaries and the cell midpoints. However, since $i = 1, \ldots, N$ and $k = 0, \ldots, K-1$, Eq. (119) represents $K \times N$ linear algebraic equations in $2K \times N$ unknown angular radiation intensities at the cell boundaries and midpoints. (Incident radiation intensities at the outer surfaces of the slab, τ_0 and τ_K, are assumed known from the boundary conditions.) Thus, to solve Eq. (119) for the radiation intensities it is first necessary to reduce the number of unknowns by relating the cell-centered intensities $I_i(\tau_{k+1/2})$ to the mesh boundary values. This reduction can be performed in a number of ways, but the simplest and most commonly used method is to assume that

$$I_i(\tau_{k+1/2}) = \frac{I_i(\tau_k) + I_i(\tau_{k+1})}{2}. \tag{120}$$

Now there are as many linear equations as unknown radiation intensities.

The solution of Eqs. (119) and (120) for the radiation intensities is complicated by the fact that the source term $Q_i(\tau_{k+1/2})$ generally depends on the radiation intensities [see Eq. (117)]. For small K and N, these linear equations can be solved directly. However, it is usual to use an iterative solution scheme which is especially applicable to more complicated cases in curved multidimensional geometry. This iterative solution is begun by guessing an initial value for the source Q_i at each spatial cell midpoint. Then substitution of Eq. (120) into (119) allows one to eliminate the cell-centered intensities and to solve for $I_i(\tau_{k+1})$ in terms of $I_i(\tau_k)$ as

$$I_i(\tau_{k+1}) = \frac{1 - \Delta\tau_k/2\omega_i}{1 + \Delta\tau_k/2\omega_i} I_i(\tau_k) + \frac{\Delta\tau_k}{\omega_i(1 + \Delta\tau_k/2\omega_i)} Q_i(\tau_{k+1/2}), \tag{121}$$

or for $I_i(\tau_k)$ in terms of $I_i(\tau_{k+1})$ as

$$I_i(\tau_k) = \frac{1 + \Delta\tau_k/2\omega_i}{1 - \Delta\tau_k/2\omega_i} I_i(\tau_{k+1}) - \frac{\Delta\tau_k}{\omega_i(1 - \Delta\tau_k/2\omega_i)} Q_i(\tau_{k+1/2}). \tag{122}$$

These two results then permit the evaluation of the intensities at all internal mesh boundaries by starting at one of the slab surfaces (where the inward intensities are specified) and sweeping inward along the direction of photon travel (constant ω_i) from mesh boundary to mesh boundary. Equation (121) is used for particles streaming to the right ($\omega_i > 0$) starting with the given $I_i(\tau_0) \equiv I_i(0, \omega_i)$ and evaluating successively $I_i(\tau_1)$, $I_i(\tau_2)$, ..., $I_i(\tau_K)$. Similarly, Eq. (122) is used for particles streaming to the left ($\omega_i < 0$) starting with the incident $I_i(\tau_K) \equiv I(\xi, \omega_i)$ and successively computing $I_i(\tau_{K-1})$, $I_i(\tau_{K-2})$, ..., $I_i(0)$. Once the radiation intensities in all directions have been found at all cell boundaries, the cell-centered intensities are computed from Eq. (120) and new and improved estimates of the sources $Q_i(\tau_{k+1/2})$ are computed from Eq. (117). This procedure of iteratively computing the radiation intensities from Eqs. (121) and (122) and then a revised source estimate from Eq. (117) is continued until the computed radiation intensities converge.

The incident boundary intensities $I_i(\tau_0 = 0)$, used to begin the forward sweep, and $I_i(\tau_K = \xi)$, used to begin the backward sweep, are obtained from the boundary conditions, Eqs. (97) and (98), as

$$I_i(0) = f_i - 2\alpha_1 \sum_{j=1+N/2}^{N} w_j \, \omega_j \, I_j(0), \qquad i = 1, \ldots, \frac{N}{2}, \tag{123}$$

and

$$I_i(\xi) = g_i + 2\alpha_2 \sum_{j=1}^{N/2} w_j \, \omega_j \, I_j(\xi), \qquad i = \frac{N}{2} + 1, \ldots, N. \tag{124}$$

Here $\omega_1, \omega_2, \ldots, \omega_{N/2}$ are positive and are the directions of the forward sweep. Ordinates $\omega_{M/2+1}, \ldots, \omega_N$ are negative and are the directions used in the backward sweep.

Various procedures can be used to accelerate the convergence and so to reduce the number of iterations required [Duderstadt and Martin 1979; Lewis and Miller 1984]. This reduction in the number of iterations for convergence is particularly important for large problems involving many mesh cells and discrete directions as would be encountered in large multidimensional problems. Moreover, the number of mesh cells and the number of discrete ordinates needed to give an adequate result are not independent. From Eqs. (121) and (122) it is seen that to ensure the left-hand side is always positive, the mesh spacing and the discrete ordinates must always be chosen such that $|\Delta\tau_k / 2\omega_i| < 1$. Thus, the maximum cell width $\Delta\tau_k$ is controlled by the smallest cosine of the polar angle, $\min |\omega_i|$ (namely, the direction closest to $\pi/2$). If more discrete directions are used, the number of spatial cells needed will generally increase. For problem geometries many mean-free-path lengths thick, as are typically encountered in shielding problems, the number of spatial cells may consequently become very large.

Although discrete-ordinates methods are widely used for radiative transfer calculations, these methods do have their limitations. Most restrictive is the requirement that the problem geometry must be one of the three basic geometries (rectangular, spherical, or cylindrical) with boundaries placed perpendicular to a coordinate axis. Problems with irregular boundaries and material distributions are difficult to solve accurately with the discrete-ordinates method. In multidimensional geometries, the discrete-ordinates method often produce spurious oscillations in the spatial distribution of the calculated intensities (the *ray effect*) as an inherent consequence of the angular discretization. Finally, the discretization of the spatial and angular variables introduces numerical truncation errors, and it is necessary to use sufficiently fine angular and spatial meshes to obtain intensities that are independent of the mesh size.

9.2 Multi-Flux Methods

Several methods, collectively called *flux methods* have been developed [Houf, 1978] whereby the continuous variation of intensity with direction, as inherent in the RTE, is approximated by the flow of radiation in discrete solid-angle segments. Widely used is the two-flux method [Schuster, 1960] and the six-flux method [Chu and Churchill, 1955]. Here we develop the general N-flux method in plane geometry.

The total solid angle at any optical depth is divided into N contiguous ranges $\Delta\Omega_i$, $i = 1, \ldots, N$, where for plane geometry, the ith range is defined as

$$\Delta\Omega_i : \omega_i \le \omega \le \omega_{i-1}, \quad 0 \le \psi \le 2\pi, \quad i = 1, \ldots, N, \tag{125}$$

where $\omega_0 = 1$ and $\omega_N = -1$. The radiation intensity is then assumed isotropic (independent of ω) within each subinterval and is denoted by $I_{i-1/2}(\tau)$. Integration of Eq. (113) over the ith solid angle range yields

$$\frac{\omega_{i-1} + \omega_i}{2} \frac{dI_{i-1/2}(\tau)}{d\tau} + I_{i-1/2}(\tau) = \gamma_s \sum_{j=1}^{N} \frac{p_{ji}}{\omega_{i-1} - \omega_i} I_{j-1/2} + \gamma_a B, \quad i = 1, \ldots, N, \tag{126}$$

where

$$p_{ji} \equiv \int_{\omega_j}^{\omega_{j-1}} d\omega' \int_{\omega_i}^{\omega_{i-1}} d\omega \, p(\omega' \to \omega). \tag{127}$$

If the phase function $p(\omega' \to \omega)$ is also assumed constant within each angular subinterval interval of ω' and ω, then

$$p_{ji} \simeq (\omega_{j-1} - \omega_j)(\omega_{i-1} - \omega_i) p(\omega_{j-1/2} \to \omega_{i-1/2}), \tag{128}$$

where $\omega_{j-1/2} \equiv (\omega_{j-1} + \omega_j)/2$ and $p(\omega_{j-1/2} \to \omega_{i-1/2})$ is computed numerically from the azimuthally-averaged phase function of Eq. (94). Finally, substitution of Eq. (128) into Eq. (126) gives the *flux equations* for solid angle segments $i = 1, \ldots, N$.

$$\boxed{\omega_{i-1/2} \frac{dI_{i-1/2}(\tau)}{d\tau} + I_{i-1/2}(\tau) = \gamma_s \sum_{j=1}^{N} (\omega_{j-1} - \omega_j) p(\omega_{j-1/2} \to \omega_{i-1/2}) I_{j-1/2} + \gamma_a B.} \tag{129}$$

The flux equations can be written equally well (and usually are) in terms of the radiant fluxes

$$J_i(\tau) \equiv 2\pi \int_{\omega_i}^{\omega_{i-1}} d\omega \, I(\tau, \omega) \simeq \pi(\omega_{i-1}^2 - \omega_i^2) I_i(\tau). \tag{130}$$

However, we choose to use the intensities so as to show the similarity between the flux equations and the discrete-ordinates (DO) equations. Comparing the DO equations, Eqs. (116) and (117), to the flux equations, Eq. (129), we see that they are identical if the DO quadrature weights w_i and ordinates ω_i are replaced by $(\omega_{i-1} - \omega_i)$ and $\omega_{i-1/2}$, respectively. In effect, the multi-flux method uses a trapezoid integration approximation to evaluate the scattering source term, whereas the DO method uses an arbitrary numerical quadrature set to evaluate the scattering integral and, hence, is more general and potentially more accurate.

In the limit of a large number of discrete directions, both models will, of course, converge to the correct result. Moreover, the same numerical solution technique used for the DO equations (i.e., the iterative, inward-outward sweep) is directly applicable to the multi-flux equations. Because of the inherent better accuracy of the DO method (for the same number of discrete directions N) compared to the flux method, the DO should always be used.

9.3 Differential or Diffusion Approximation

In many radiative transfer problems the angular dependence of the radiation intensity is not required; rather, the angularly integrated intensity $\Phi(\mathbf{r}) \equiv \int_{4\pi} d\Omega\, I(\mathbf{r}, \mathbf{\Omega})$ is all that is needed. To obtain an equation for Φ, integrate the RTE over all directions. The resulting equation involves not only Φ but also the flux vector $\mathbf{J}(\mathbf{r}) = \int_{4\pi} d\Omega\, \mathbf{\Omega} I(\mathbf{r}, \mathbf{\Omega})$. To obtain an equation for $\mathbf{J}$, multiply the RTE by $\mathbf{\Omega}$ and integrate over all directions. However, the result not only depends on $\mathbf{J}$ but also on a higher angular moment. To approximate this higher moment, $I(\mathbf{r}, \mathbf{\Omega})$ is assumed to vary linearly with $\mathbf{\Omega}$. Combining these two moment equations to eliminate $\mathbf{J}$, yields [Shultis and Faw, 1996]

$$-\nabla \bullet D_\nu \nabla \Phi_\nu(\mathbf{r}) + \mu_a(\nu)\Phi_\nu(\mathbf{r}) = 4\pi \mu_a(\nu) B_\nu(T) \tag{131}$$

where the *diffusion coefficient* is

$$D_\nu(\mathbf{r}) = \frac{1}{3[\mu_e(\mathbf{r}, \nu) - \varpi_o \mu_s(\mathbf{r}, \nu)]}. \tag{132}$$

In this result ϖ_o is the mean cosine of the scattering angle, i.e.,

$$\varpi_o(\nu) = \int_{-1}^{1} \omega_s\, \overline{p}(\nu, \omega_s)\, d\omega_s. \tag{133}$$

For the plane-geometry azimuthally-symmetry problem considered in this section, the differential approximation of Eq. (131) can be expressed in terms of the optical depth τ, where $d\tau = \mu_e\, dx$, as

$$\boxed{-\frac{d}{d\tau}\overline{D}(\tau)\frac{d\Phi(\tau)}{d\tau} + \gamma_a \Phi(\tau) = 4\pi\gamma_a B(T),} \tag{134}$$

where again the frequency subscript is suppressed and the modified diffusion coefficient $\overline{D} \equiv \mu_e\, D$, i.e.,

$$D(\tau) = \frac{1}{3[1 - \gamma_s \varpi_o]}, \tag{135}$$

and the angularly-integrated intensity (zeroth moment) is

$$\Phi(\tau) = 2\pi \int_{-1}^{1} d\omega\, I(\tau, \omega). \tag{136}$$

Boundary conditions for the angularly integrated intensity may be obtained from Eqs. (97) and (98). Multiplication of these equations by $2\pi\omega$, integration over the directions into the medium, and use of the P_1 approximation [$2\pi \int_0^{\pm 1} d\omega\, \omega I(\tau, \omega) \simeq \frac{\Phi(\tau)}{4} \mp \frac{\overline{D}}{2}\frac{d\phi(\tau)}{d\tau}$] gives [Khalil 1980]

$$\overline{D}(0)\frac{d\Phi(0)}{d\tau} - \frac{1 - \alpha_1}{2(1 + \alpha_1)}\Phi(0) = \frac{2\pi}{1 + \alpha_1}\int_0^1 d\omega\, \omega\, f(\omega) \tag{137}$$

$$\overline{D}(\xi)\frac{d\Phi(\xi)}{d\tau} + \frac{1 - \alpha_2}{2(1 + \alpha_2)}\Phi(\xi) = -\frac{2\pi}{1 + \alpha_2}\int_{-1}^0 d\omega\, \omega\, g(\omega). \tag{138}$$

9.3.1 Numerical Solution

Although Eq. (134) can be solved analytically in a piecewise homogeneous medium provided $T(\tau)$ is known, it is usually much easier to obtain the solution numerically. Towards this end, the optical thickness ξ is divided into $N-1$ contiguous subintervals by N equally spaced nodes τ_k. Integration of Eq. (134) over the thickness Δ of one subinterval centered about each interior node (i.e., $k = 2, 3, \ldots, N-1$) and approximation of the derivatives by first-order finite differences, yields [Khalil, 1980]

$$a_{k,k-1}\Phi_{k-1} + a_{k,k}\Phi_k + a_{k,k+1}\Phi_{k+1} = S_k, \qquad k = 2, \ldots, N-1 \tag{139}$$

where

$$a_{k,k-1} \equiv -\overline{D}_{k-1/2}, \quad a_{k,k+1} \equiv -\overline{D}_{k+1/2}, \quad a_{k,k} \equiv \overline{D}_{k-1/2} + \overline{D}_{k+1/2} + \frac{\Delta^2}{2}(2 - \omega_{k+1/2} - \omega_{k-1/2}), \tag{140}$$

$$\S_k \equiv \frac{4\pi}{\Delta}\int_{\tau_{k-1/2}}^{\tau_{k+1/2}} d\tau\, \gamma_a B[T(\tau)] \simeq 4\pi\gamma_a(\tau_k)B[T(\tau_k)], \tag{141}$$

and

$$\Phi_k \equiv \frac{1}{\Delta}\int_{\tau_{k-1/2}}^{\tau_{k+1/2}} d\tau\, \Phi(\tau). \tag{142}$$

Equations (139) are $N-2$ algebraic equations in the N unknowns $\Phi_1, \ldots, \Phi_N$. The needed two extra equations are obtained by integrating the boundary conditions, Eqs. (137) and (138) over the half-cells adjacent to the boundaries. These boundary node equations have the form

$$a_{1,1}\Phi_1 + a_{1,2}\Phi_2 = S_1 \qquad \text{and} \qquad a_{N,N-1}\Phi_{N-1} + a_{N,N}\Phi_N = S_N. \tag{143}$$

The discretized Eqs. (139) and (143) can be written in matrix form $\mathbf{A\Phi} = \mathbf{S}$ where the matrix $\mathbf{A}$ is tridiagonal. This set of equations is readily solved by direct elimination (using the tridiagonal matrix algorithm).

10 Example: Particle Suspensions

As an illustration of the methods used for radiative transfer in interacting media, we consider the case of stationary radiative transfer in a reacting particle suspension (see Fig. 13). Burning spherical coal/char particles are suspending uniformly in an oxidizing gas (primarily O_2). If we assumed the particle suspension is grey, the RTE, Eq. (111), is

$$\omega\frac{\partial I(\tau,\omega)}{\partial\tau} + I(\tau,\omega) = \gamma_s(\tau)\int_{-1}^{1} d\omega'\, p(x,\omega'\to\omega)I(x,\omega') + \gamma_a(\tau)\frac{\sigma T^4[T(\tau)]}{\pi}. \tag{144}$$

The temperature profile is related to the radiation field, under an assumption of local radiative equilibrium (see Eq. (112)) which can be written as

$$\sigma T^4(\tau) = \frac{\pi}{2}\int_{-1}^{1} d\omega\, I(\tau,\omega) + \frac{1}{4\mu_a}S_{ex}(\tau,T). \tag{145}$$

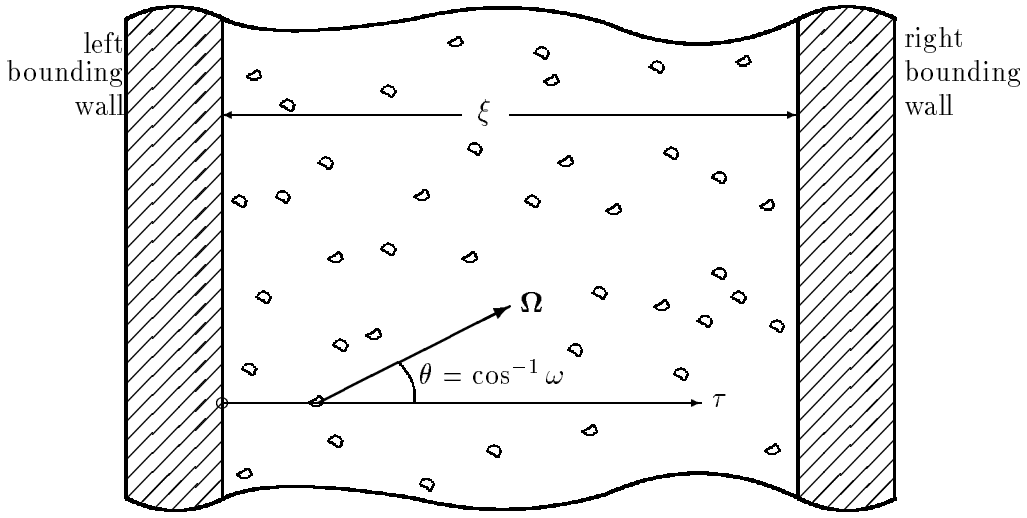

Figure 13. Geometry for a coal/char suspension between two parallel bounding walls. The left wall has temperature T_1 and isotropic reflectivity $alpha_1$ while the corresponding right-wall parameters and T_2 and $alpha_2$.

10.1 Heat Generation Model

In this section we review a heat generation model, which, although somewhat simplistic, exhibits many features expected of realistic models. It is assumed that the heat generation rate S_{ex} is determined exclusively by the rate of heterogeneous (solid-gas) reaction. Homogeneous (gas-gas) reactions and devolitilization are ignored. Convective and diffusive heat transfer, as well as sensible energy changes, are assumed negligible compared to radiative heat transfer rates. For such a combustion model, the heat generation rate is given by [Khalil, 1980]

$$S_{ex} = P\Delta h \frac{S}{K_d^{-1} + K_s^{-1}}. \tag{146}$$

Here P is the partial pressure of the oxygen, Δh is the energy released per unit mass of the fuel consumed, and S is the surface area of the particles per unit volume, which is related to the bulk density ρ_p and diameter d_p of the particles by

$$S = \frac{6\rho_p}{d_p \rho_c} \tag{147}$$

where ρ_c is the density of the coal/char. The quantities K_d and K_s are the oxygen diffusion rate and surface reaction rate coefficients, respectively, and are given by [Field et al. 1967]

$$K_d = \frac{48 D_o T^{0.75}}{R T_o^{1.75} d_p} \qquad \text{and} \qquad K_s = Z e^{-E/RT}, \tag{148}$$

where T is the temperature of the medium (the gases and solids are assumed to be in thermal equilibrium), D_o is the diffusivity of the oxygen in air at temperature T_o, R is the universal gas

constant, Z is the pre-exponential factor (assumed independent of temperature), and E is the activation energy. The expression for the diffusional rate coefficient K_d assumes that oxygen is conserved in the particle boundary layer, i.e., consumption of oxygen occurs either at the particle surface or relatively far from it.

The local radiative equilibrium relation, Eq. (145), can be cast into dimensionless form by defining $T^* \equiv E/R$, $\Phi^* \equiv \sigma T^{*4} = \sigma(E/R)^4$, $\widehat{T} \equiv T/T^*$, and $\Psi \equiv \frac{\pi}{2\Phi^*}\int_{-1}^{1} d\omega\, I(\tau,\omega)$. Division of Eq. (145) by Φ^* yields

$$\widehat{T}^4(\tau) = \Psi(\tau) + \frac{A}{(2\widehat{T})^{-0.75} + B\exp(1/\widehat{T})}, \tag{149}$$

where A and B are dimensionless constants defined as

$$A = \frac{P\Delta h}{\sigma(E/R)^4}\left(\frac{4S}{\mu_a}\right)\frac{48D_o(T^*/T_o)^{0.75}}{RT_o d_p} \qquad \text{and} \qquad B = \frac{48D_o(T^*/T_o)^{0.75}}{ZRT_o d_p}. \tag{150}$$

Representative values are: activation energy E = 146 kJ/mol, preexponential factor Z = 500 mol/(cm^2 s atm) = 5.92 kg/(N s), oxygen diffusivity D_o = 3.49 cm^2/s at T_o = 1600 K, and $P\Delta h$ = 250 atm cal/g. With these constants (and the optical properties presented in the next section), a monodisperse suspension of 50 μm diameter spherical coal particles, with a bulk density $\rho_p = 10^{-4}$ g/cm^3 and a particle density of 1.5 g/cm^3, generates heat at a rate of 1 W/cm^3 at a temperature of 1750 K. This power density of 1 W/cm^3 is typical of the thermal loading in the primary heat release zones of pulverized fuel boilers [Richter and Heap 1981; Field et al. 1967]. With these values for the various model parameters, the dimensionless parameters A and B become 2.014×10^{-4} and 1.805×10^{-4}, respectively.

For the above parameterization, the heat generation rate per unit volume of the suspension becomes

$$S_{ex} = 4\mu_a\sigma(E/R)^4\frac{A}{(2\widehat{T})^{-0.75} + B\exp(1/\widehat{T})} = 3.522\times 10^4\frac{A}{(2\widehat{T})^{-0.75} + B\exp(1/\widehat{T})} \ \text{W/cm}^3 \tag{151}$$

where $\widehat{T} = T/(E/R) = T/17{,}561$. This heat generation function is shown in Fig. (14).

It should be noted that other more sophisticated heat-generation rate models are readily incorporated into the analysis that follows. For example, Khalil [1980] has added a term to account for heat conduction between the burning particles and the ambient gas, which generally have different temperatures (our analysis assumes the gas and particles have the same temperature). The above model, while based on several simple assumptions, is not unrealistic and yields results that agree reasonable well with experimental observations.

10.2 Optical Properties of the Suspension

The extinction and scattering coefficients are computed from $\mu_e = F_e S/4$ and $\mu_s = F_s S/4$, respectively, where F_e is the *extinction efficiency* and F_s is the *scattering efficiency*. The extinction and scattering efficiencies are calculated from Mie theory given the particle size parameter α ($= \pi d_p/\lambda$, where λ is the radiation wavelength), and the complex refractive index of the particles, m. The wavelength at which the maximum radiation intensity occurs at combustion temperatures is roughly 2 μm, and the typical size of pulverized coal is between 10 and 100 μm. The particle size parameter, α, thus falls in the range of 10 to 150.

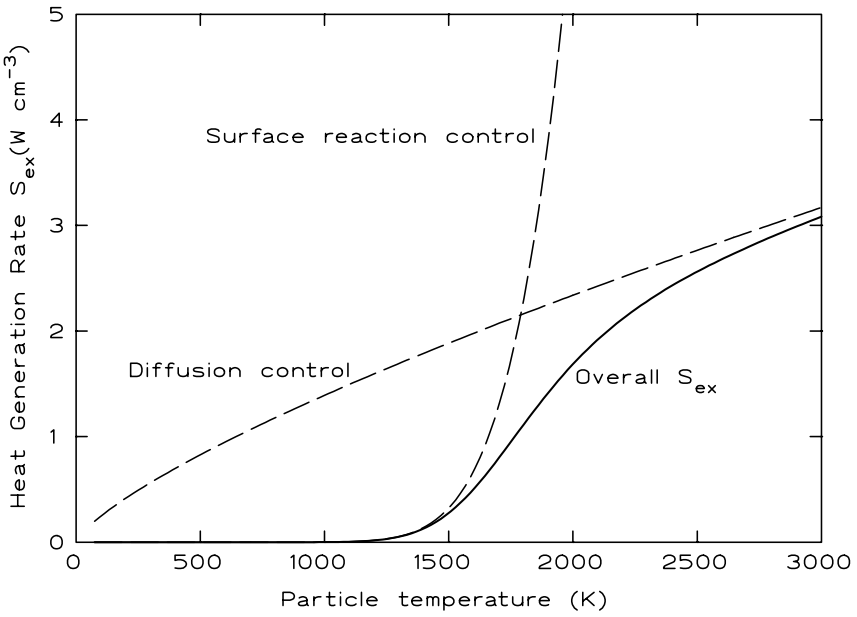

Figure 14. The heat generation model for a burning carbonaceous particle suspension. Also shown are the limiting values for oxygen diffusion control and the surface reaction control.

In this range, the scattering and extinction efficiencies are weak functions of the size parameter, and diffracted radiation is concentrated within a narrow angle about the incident direction. Treatment of the diffracted radiation as purely forward scattering allows this effect to be neglected entirely by subtracting its contributions from the extinction and scattering efficiencies. The scattering phase function is thus determined entirely by the reflected component of the scattering radiation and may be written for opaque and diffusely reflecting particles as

$$p(\theta_s) = \frac{2}{3\pi^2}(\sin\theta_s - \theta_s \cos\theta_s) \qquad (152)$$

where $\cos\theta_s = \mathbf{\Omega}\cdot\mathbf{\Omega}'$. For a simpler isotropic scattering model, the phase function $p = 1/4\pi$.

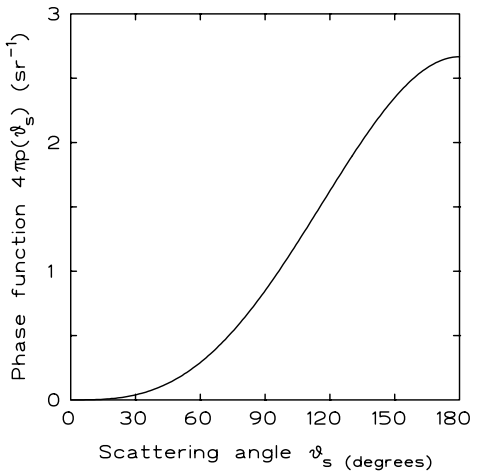

Figure 15. Phase function of Eq. (152).

The complex refractive index of carbonaceous solids, particularly coals is not well known. For pyrolytic graphite, soot, and coal in the wavelength region between 1 to 5 μm, the refractive index has a real part between 1.5 to 3 and an imaginary part of from 0.1 to 1.0. For calculations is this section, we assume $m = 1.93(1 - i0.53)$, close to the recommended value of $m = 2 - i$ for coal dust between 350 and 1,000 nm [Janzen 1979].

For $d_p = 50$ μm, $m = 1.93(1-0.53i)$ and $\lambda = 2$ μm, the size parameter $\alpha = 78.54$, the extinction efficiency $F_e = 1.117158$, and the scattering efficiency $F_s = 0.300529$. The absorption efficiency $F_a = F_e - F_s = 0.816629$ and $\gamma_s = 0.269$. For the pulverized coal suspension considered in the previous section, $S = (6\rho_p)/(d_p\rho_c) = 0.08$ cm^{-1}. Finally, the optical interaction coefficients are found from $\mu_i = F_i S/4,\ i = e, a, s$ so that $\mu_e = 0.0223$ cm^{-1}, $\mu_a = 0.0163$ cm^{-1}, and $\mu_s = 0.00601$ cm^{-1},

10.3 Solution Algorithm

To obtain a radiation field $I(\tau,\omega)$ and a particle temperature profile $T(\tau)$ that satisfy both the RTE, Eq. (144), and the local radiative equilibrium condition of Eq. (145), the following iterative procedure can be used.

1. Guess an initial temperature profile, i.e., $T(\tau_k),\ k = 0, 1, \ldots, K$. Typically, one assumes a constant profile, e.g., $T = 1500$ K. Then calculate $Q_i(\tau_{k+1/2})$ from Eq. (117) assuming $I = 0$.

2. Solve the RTE by the method of discrete ordinates using the inward-outward sweep of Eqs. (121) and (122). To start these sweeps, the inward radiation at the boundaries must first be evaluated from Eqs. (123) and (124).

3. With the new estimate of the radiation intensity I or $\Psi(\tau)$, obtain a revised temperature profile by solving Eq. (145) for $T(\tau)$ or Eq. (149) for $\widehat{T}(\tau)$. The non-linear equations for T or $\widehat{T}$ have either one or three solutions. The physical realistic solution can be found by the following iteration scheme based on Eq. (149):

$$\widehat{T}^{(\ell+1)}(\tau) = \left[\Psi(\tau) + \frac{A}{(2\widehat{T}^{(\ell)})^{-0.75} + B\exp(1/\widehat{T}^{(\ell)})}\right]^{0.25}, \tag{153}$$

   starting with a sufficiently high value of $\widehat{T}^{(0)}$. If there is only one solution, any starting value may be used. If there are three solutions, the largest $\widehat{T}$ is sought and a starting value greater than the first two roots is needed [Khalil, 1980].

4. Update the source term $Q_i(\tau_{k+1/2})$ from Eq. (117) using the new temperature profile.

5. Repeat steps $2-4$ until the radiation and temperature fields converge.

10.4 Example Results

To illustrate the models and methodology described in this section, a few illustrative results are presented. The model parameters, unless otherwise stated, are those presented above.

Figure 16 shows the temperature profile is a suspension bounded by vacuum walls (i.e., no radiation is incident on the suspension). One profile is for a constant heat generation rate $S_{ex} = 1$ W/cm^3, and the other is for the heat generation model of Eq. (151).

Figure 17 shows the maximum temperature in a suspension bounded by vacuum walls for different suspension thicknesses Notice that if the suspension becomes too thin, the temperature suddenly falls to near zero, an indication that the radiant energy leakage through the walls becomes too great that not enough radiant energy is retained to sustain combustion. It is seen that the thickness required for such *stationary ignition* is very sensitive to the activation energy E. The ignition point is also very sensitive to other problem parameters such as boundary emissivities and reflectivities.

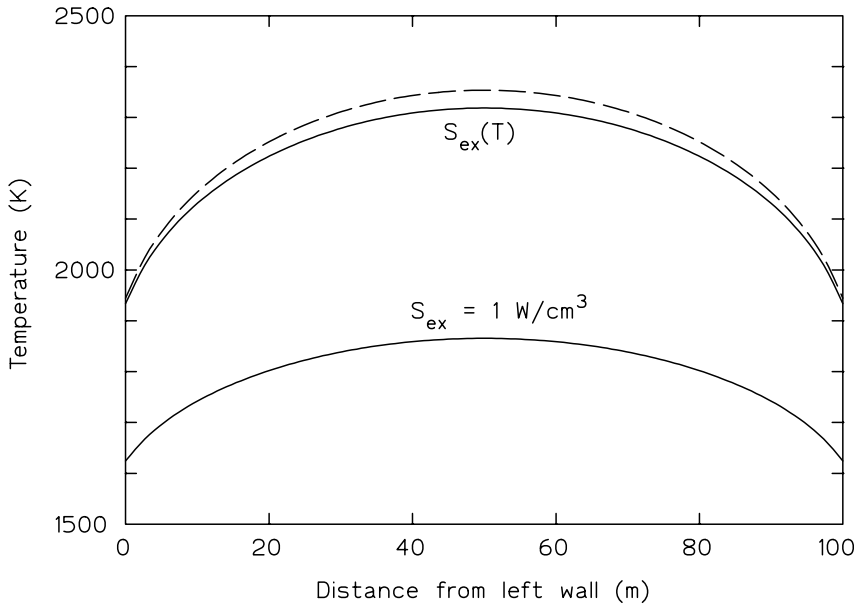

Figure 16. Temperature profiles in a burning coal suspension of optical thickness 2.234 (1 m) bounded by vacuum walls. One profile is for a suspension with a uniform power density of 1 W/cm^3 (bottom profile) and for the model of Eq. (151) (top profile). Solid curves are for isotropic scattering and the dashed curve is for the anisotropic phase function of Eq. (152).

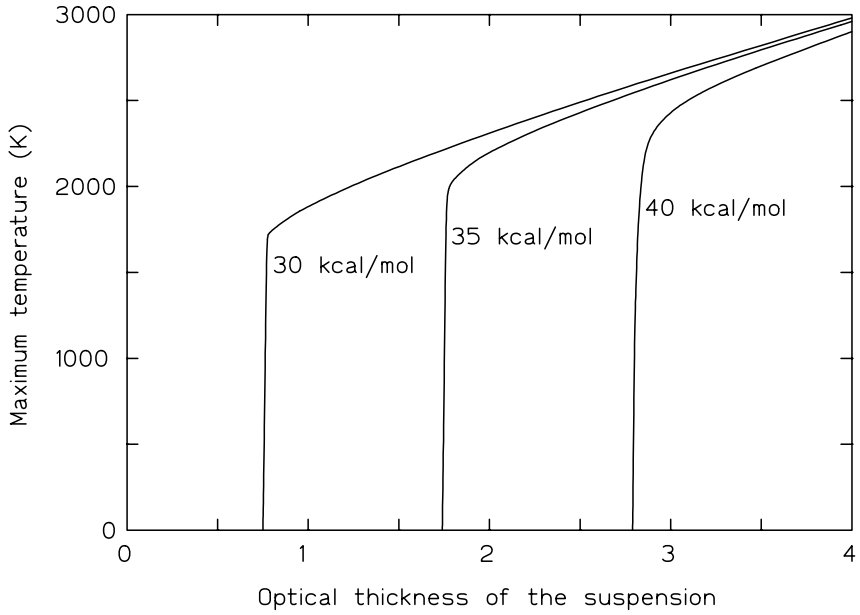

Figure 17. Maximum temperature in a burning coal suspension bounded by vacuum boundaries for three values of the activation energy E. If the suspension is too thin, combustion cannot be maintained. Isotropic scattering is assumed.

REFERENCES

CARLSON, B.G. AND K.D. LATHROP, "Transport Theory, the Method of Discrete Ordinates," in *Computing Methods in Reactor Physics*, H. Greenspan, C.N. Kelber, and D. Okrent (eds.), Gordon and Breach, New York, 1968.

CASE, K.M., AND P.F. ZWEIFEL, *Linear Transport Theory*, Addison-Wesley, Reading, MA, 1967.

CHANDRASEKHAR, S., *Radiative Transfer*, Dover, New York, 1960.

DUDERSTADT, J.J., AND W.R. MARTIN, *Transport Theory*, Wiley, New York, 1979.

ESSENHIGH R.H., "Combustion and Flame Propagation in Coal Systems: A Review," *Sixteenth International Symposium on Combustion*, p. 353, The Combustion Institute, 1977.

FIELDS, M.A., D.W. GILL, D.B. MORGAN, and P.D.W. HAWKSLEY, *Combustion of Pulverized Coal*, The British Coal Utilization Research Assoc., Leatherhead, Surrey, England, 1967.

JANZEN, J., "The Refractive Index of Colloidal Carbon," *J. Colloid and Interface Sci,*, **69**, p.!436, 1979.

KHALIL H., *Radiative Transfer in Pulverized Coal Suspensions*, MS Thesis, Kansas State University, Manhattan, KS, 1980.

KHALIL H., J.K. SHULTIS, and T.W. Lester, "Comparison of Three Numerical Evaluation Methods for Evaluation of Radiant Energy Transfer in Scattering and Heat Generating Media," *Numerical Heat Transfer*, **5**, p. 235, 1982.

KHALIL H., J.K. SHULTIS, and T.W. Lester, "Stationary Thermal Ignition of Particle Suspensions," *J. Heat Transfer*, **105**, p. 288, 1983.

LEWIS, E.E., AND W.F. MILLER, *Computational Methods of Neutron Transport Theory*, Wiley, New York, 1984.

RICHTER, W. and M.P. HEAP, "The Impact of Heat Release Pattern and Fuel Properties on Heat Transfer in Boilers," ASME Paper 81-WA/HT-27.

SANCHEZ, R., AND N.J. MCCCORMICK, "A Review of Neutron Transport Approximations," *Nucl. Sci. Eng.*, **80**, 481–535, (1982).

SHULTIS, J.K. AND R.E. FAW, *Radiation Shielding*, Prentice Hall, Upper Saddle River, NJ, 1996.

SIEGEL, R. AND J.R. HOWELL, *Thermal Radiation Heat Transfer*, 3rd ed., Hemisphere Publ., Washington, 1992.

STEWART, J.C., "Some Topics in Radiative Transfer," in *Developments in Transport Theory*, E. Inönü and P.F. Zweifel, Eds., Academic Press, New York, 1967.